NASA TN D-297

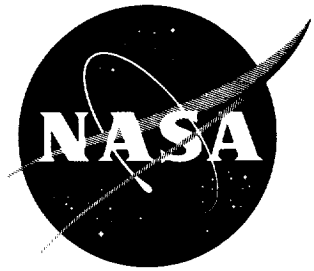

TECHNICAL NOTE

D-297

MEASUREMENT OF SCREEN-SIZE EFFECTS ON INTENSITY, SCALE, AND SPECTRUM OF TURBULENCE IN A FREE SUBSONIC JET

By Charles D. Howard and James C. Laurence

Lewis Research Center
Cleveland, Ohio

NATIONAL AERONAUTICS AND SPACE ADMINISTRATION

WASHINGTON August 1960

NATIONAL AERONAUTICS AND SPACE ADMINISTRATION

TECHNICAL NOTE D-297

MEASUREMENT OF SCREEN-SIZE EFFECTS ON INTENSITY, SCALE, AND SPECTRUM OF TURBULENCE IN A FREE SUBSONIC JET

By Charles D. Howard and James C. Laurence

SUMMARY

The results are reported of hot-wire anemometer measurements of the fluctuating longitudinal component of the turbulent velocities in the mean flow downstream of screens in an air jet. These measurements have been analyzed by well-established techniques to give the influence of the screen mesh size on the turbulent intensity, scale, and the power-spectral-density. The results show a linear dependence of the intensity upon the screen mesh size for locations within the central core of the air jet.

The spectral-density curves show that the screens redistribute the turbulent energy from the low frequencies (<1000 cps) to the high frequencies (>1000 cps). The effects of the screens are overwhelmed in the mixing region of the jet flow by the turbulence levels existing there.

The large pressure drops occurring across the screens reduce the velocity of the jet as compared to the jet without screens by approximately one-third for the velocity and range of mesh sizes investigated and reported in this report. The turbulence scale is a linear function of distance from the nozzle exit and is somewhat greater than comparable jets without screens.

INTRODUCTION

In the field of aerodynamic noise the relation between the noise output of a jet of air (turbojet engine) and the turbulence in the airflow has been considered by Lighthill (ref. 1) and others (refs. 2 to 5). Experimental evidence exists (ref. 6) which shows that the turbulence levels within the jet are influenced by the initial turbulence in the airstream. While these initial levels are low in jets which result from the expansion of air from a plenum through a large area contraction to the atmosphere (ref. 7), they may not be low in other configurations. For example, in the case of a ducted-fan jet engine the noise levels produced by the concentric jets are larger than those predicted from model studies. Studies of concentric jets (refs. 8 and 9) have shown that the

sound power should be equal to or somewhat less than that produced by two circular jets with the same areas and velocities of the concentric jets. In the model studies, however, the initial turbulence of the jets is quite low. In the ducted-fan engine both the fan and primary jets may well have high initial turbulence levels. The fan air has very little convergence to reduce turbulent intensities, and the fan and turning vanes may well produce large flow fluctuations. The primary jet may also have much larger initial turbulent intensities than a straight turbojet since the flow convergence after the last turbine is much less than for a straight turbojet. As a first guess it would appear that increases in turbulence of the primary jet would be most important since its exit velocity is much higher (1.5 or more times the secondary flow).

It is probable that the lack of agreement between the predicted and measured noise levels in the fan engine is the result of the increased initial level of turbulence in the jets. Since these fan engines are to be introduced in large numbers in transport aircraft, the relation between the turbulence levels and the noise output is of compelling interest.

Dryden and his associates (ref. 10) investigated the effect of placing screens into an airstream. They found that the insertion of the screens makes the flow turbulent since eddies are shed from the wires forming the mesh. The initial size and intensity of the eddies are determined by the dimensions of the screen. Very close to the screen the wakes from the individual wires influence the turbulence, but this effect soon disappears (within 15 mesh lengths), leaving the turbulence uniformly distributed. Since the turbulent motion decays rapidly, the intensity of turbulence decreases with distance from the screens. Hence, fine-mesh screens are often inserted in wind tunnels to distribute the turbulence uniformly and to obtain the lower level which exists after the mesh pattern has decayed.

Another instance of the effect of initial turbulence level on noise generation is the example of the use of screens as noise suppressors (ref. 11). The noise reduction which takes place as a combined result of the change in turbulence structure and the reduction in jet velocity makes screens an ideal noise suppressor for the ground runup of jet airplanes. The effect of the increase in turbulent scale and intensity in increasing the noise output of an air jet is overpowered by the accompanying decrease in mean velocity downstream of the screen. This combined effect is well illustrated by the data of references 11 and 12.

The insertion of screens in the flow, therefore, seems to be an ideal way to determine the effect of initial turbulence levels on the noise output or any of a number of other flow measurements (total pressure, static pressure, etc.). To determine, therefore, the effect of the insertion of screens into a circular jet on the turbulence parameters, the experimental program described in this report was undertaken as a part of the Aerodynamic Noise Research program at the Lewis Research Center.

SYMBOLS

D	diameter of nozzle exit
d	diameter of wire of screen
$\bar{e}$	average hot-wire bridge voltage
$e(t)$	fluctuating hot-wire bridge voltage
L_x	scale of turbulence (see eq. (1))
M	mesh size
P	total pressure
ΔP	pressure drop across screens
P_B	barometric pressure
R_x	longitudinal correlation coefficient
R_τ	autocorrelation coefficient
t	time
U_c	mean core velocity downstream of screen
U_l	local mean velocity
u'	$\sqrt{\overline{u^2}}$
u_1, u_2	longitudinal component of velocity fluctuations at points 1 and 2
x,y,z	rectangular coordinates, x in mean flow direction
τ	delay time
τ_0	delay time when $R_\tau = 0$

INSTRUMENTATION AND TEST FACILITIES

Screens, Jet Nozzle, and Air-Handling Facilities

Three screens of varying mesh sizes (see table I) were selected to evaluate their effect on certain turbulence parameters within the core of a subsonic jet. The screens and screen holders were similar in construction details (see fig. 1 for screen details). The screen wires were

interwoven into approximately the same plane. As indicated in the figure, the mesh size was taken to be from the center of one wire to the center of the next wire forming the mesh. The meshes were of commercial grade and were not exactly square in shape.

The nozzle used in these experiments was a 2-inch-diameter convergent-type nozzle shown in figure 2; a map of the flow field is given in figure 3. The nozzle was attached by means of flanges to a large plenum chamber (ref. 3) through which dry air at 40 pounds per square inch was supplied. The screen holder was bolted to the nozzle flange with the screen geometrically centered, parallel and adjacent to the nozzle lip (fig. 4).

The airflow through the nozzle and screens is controlled by means of automatically adjusted and remotely controlled valves ahead of the plenum. The total pressure and temperature of the air are measured by a total head tube and thermocouple placed in the plenum. A 3/4-inch felt filter ensures a clean air supply and protects the hot wires from damage.

Other Instrumentation

The hot-wire anemometers used in this test were the constant-temperature type described in reference 13. The hot-wire probes were single-wire probes with the sensitive element a 0.080-inch-long by 0.002-inch-diameter tungsten filament. The mounting procedure is an adaptation of the plating-soldering technique used at the National Bureau of Standards (ref. 14).

The data processing instrumentation consisted of a special series of instruments designed and built at the Lewis Research Center (ref. 15) and commercially available instruments. Examples of the former are the autocorrelator, which used signals recorded on magnetic tape to obtain the autocorrelograms.

A Brüel and Kjaer audiospectrum analyzer and level recorder with 34 filters, 1/3-octave bandwidth recorded the spectrum level of the signals. The frequency range of the instrument is from 16 to 35,000 cycles per second (center frequency of the 1/3-octave bands).

The root-mean-square of the fluctuating voltages was read with a Ballantine True R.M.S. Voltmeter Model 520, and the mean-square output of this meter was recorded continuously on a strip chart.

EXPERIMENTAL PROGRAM

Data Collection

In view of the twofold objective of this program: (1) to determine the effect of the initial turbulence level on certain turbulence parameters and (2) to control or predict the turbulence parameters in the central core of an air jet in which screens are placed, the experimental program was planned as follows: In a suitable air jet, a series of screens were placed at the nozzle exit, and turbulence measurements were made. These measurements were made by hot-wire anemometer techniques which have been highly developed at the Lewis Research Center (refs. 6 and 12). A block diagram is given in figure 5, which shows the instrumentation setup that was designed to reduce the time required for data taking.

The first part of the experimental procedure was the recording of the hot-wire bridge voltage both direct current (d.c.) and alternating current (a.c.) as a function of probe position in the flow field. At a given longitudinal position in the jet (x/D), the probe was set into motion in the z/D direction (y/D = 0) by means of the probe positioning and indicating apparatus. The d-c part of the bridge voltage was recorded by one pen of the strip-chart recorder as the probe was driven to traverse the jet. The a-c bridge voltage was squared and averaged by the true rms meter and recorded by the second pen of the recorder. With appropriate calibration of these voltage signals the intensity of turbulence and the local mean velocity profiles can be calculated. These profiles show the relation between the intensity of turbulence and local mean velocity and position of the probe in the flow field of the jet.

The second part of the data acquisition procedure was the recording of the fluctuating voltages for later analysis. At predetermined points in the flow field the a-c signals were recorded as a function of time on a dual-channel tape recorder. As indicated in the block diagram (fig. 5), identical signals were recorded on both channels to make possible an autocorrelation analysis of the fluctuations. At the same time the magnetic-tape recordings were being made, a spectrum analysis was accomplished by means of the audiospectrum analyzer.

Visual inspection of the a-c signals and the d-c signals was readily available by means of a cathode ray oscilloscope, true rms meter, and a d-c panel-type voltmeter. These meter readings can be recorded from time to time at each point and serve as a check on the accuracy with which the recordings (strip chart) have been made. These signals serve also as a constant monitor of hot-wire damage, changes in calibration, or breakage.

Data Processing

The data in the form of strip charts were read by means of a curve reader which punched cards for electronic data reduction according to the methods described in reference 15. These calculations gave local mean velocity and intensity of turbulence.

The magnetic-tape recordings were processed by means of an autocorrelator. The correlograms were used to obtain the scale of turbulence. The scale of the turbulence is defined by

$$L_x = \int_0^\infty R_x \, dx \tag{1}$$

where L_x is the scale in inches and R_x is the cross correlation:

$$R_x = \frac{\overline{u_1 u_2}}{\sqrt{\overline{u_1^2}}\sqrt{\overline{u_2^2}}} \tag{2}$$

and x is the separation of the two points at which the velocity fluctuations u_1 and u_2 are measured. If Taylor's hypothesis (ref. 16) can be assumed:

$$x = U_l \tau$$

(where U_l is the local mean velocity and τ is the time required for the turbulent eddy to be convected from point 1 to point 2), then

$$L_x = \int_0^\infty R_\tau U_l \, d\tau \tag{3}$$

Here R_τ is the autocorrelation coefficient:

$$R_\tau = \frac{\overline{u(t)u(t \pm \tau)}}{\sqrt{\overline{u(t)^2}}\sqrt{\overline{u(t \pm \tau)^2}}} \tag{4}$$

In equation (4) $u(t)$ and $u(t \pm \tau)$ are identical signals except that one is delayed in time with respect to the other by an amount τ.

Since the definition of turbulent scale is somewhat arbitrary, in this report only the positive area of the autocorrelograms was used in evaluating L_x. Hence, $L_x = \int_0^{\tau_0} R_\tau U_l \, d\tau$ (5) where τ_0 is the delay time where R_τ is first equal to zero.

The spectral-density curves were obtained from the audiospectrum charts as described in reference 6. The energy content in specific bands of frequencies as compared to the sum total of energy in all frequencies is well represented by the spectral-density curves. These curves are useful also to indicate resonant frequencies, flow periodicities (vortex shedding), and so forth in the airflow. And, if desired, the turbulence scale can be evaluated from these spectrograms (see ref. 6). This was not done in this report.

Accuracy of Results

A discussion of the accuracy of the measurements made with the constant-temperature hot-wire anemometer is given in references 12 and 17. In addition, a certain amount of discretion is needed in reading the averages of randomly varying fluctuating quantities.

No corrections for averaging errors due to wire length were made (see ref. 10). In the measurements reported, the scales of turbulence were greater than the wire length.

The results as a whole are as accurate as the usual hot-wire results but in any case are considered to be correct within ±10 percent.

RESULTS AND DISCUSSION

The results of the hot-wire measurements downstream of the screens in a subsonic jet are presented in a series of graphs. Since preliminary measurements showed the jet to be symmetrical with respect to the center-line, the results from only one-half of the flow are presented. Total-pressure surveys 2 inches downstream of the screens showed that the pressure drop across the screens at a Mach number of 0.3 was approximately 1 inch of mercury (see table II). With pressure drops of this magnitude the velocity downstream of the screens was 263 feet per second for the largest mesh (0.472 in.) and 277 and 244 feet per second for the other two (0.252 and 0.119 in., respectively).

Intensity of Turbulence

The intensity of turbulence was measured at stations in the flow specified by x/D, y/D, and z/D distances from the geometric centerline of the jet. The coordinate axes are shown on the photograph of the nozzle (fig. 2) and in the map of the flow field (fig. 3). Figures 6 and 7 show the results of these measurements for the three mesh sizes used in the experiments and at x/D values of 1.0, 2.0, 3.0, 4.0, and 5.0. (All surveys were made along the $y/D = 0$ axis.) In figure 6 the intensity of turbulence is given as a ratio to the mean core velocity. In general, the curves of figure 7, which are crossplots of figure 6, show that the screens have little effect on the intensity of turbulence at $x/D \approx 1.0$ and a slight increase for $x/D \approx 3.0$ and 5.0 for $z/D = 0.5$, as compared with the jet without screens (points marked * on fig. 3). For the $z/D = 0$ position (down the centerline of the jet) the effect is a small increase of intensity except for $x/D = 5.0$, where the intensity is changed by the screens about the same amount as at distances closer to the nozzle exit. The overall level, however, is greater because the flow has become completely mixed, and the core has disappeared.

These conclusions are shown even better in figure 7 where the turbulence intensity for several values of x/D and z/D is shown as a function of mesh size. From figure 7 it can be seen that the turbulence intensity is, in general, a linear function of mesh size in the central core. However, for the mixing region of the jet flow ($x/D > 3.0$, $z/D = 0.5$) this linearity does not exist. In this region of the jet flow (points marked * on fig. 3) the turbulence is fully developed. The core does not reach into this region, and the presence of the screens at the exit of the nozzle does not affect the turbulence intensity measured here as strongly as it does within the core. There are shown for reference purposes some values of the turbulence intensity for a circular nozzle with no screens. These values were taken from reference 6. In almost all cases, then, these figures show that the insertion of the screens increases the turbulence intensity in all the regions of the jet investigated; in some a great deal, in others not so much. The increase is a linear function of mesh size of the screens.

The curves of figure 8 are included as a convenience to illustrate the ratio of the intensity of turbulence to the local mean velocity. The conclusions regarding the three parts of figure 8 are obviously the same as those of figure 6 since they are the same data. The local mean velocity is measured at the measurement point, while the core velocity is measured within the core of the jet but downstream of the screens.

In figure 9 the relation of the turbulence intensity to the distance from the nozzle exit is given in terms of core velocity and local mean velocity for the three mesh sizes used. In figure 9 the intensity reaches a minimum about 2 diameters downstream and increases thereafter for all three mesh sizes. It is apparent that the effect of the screens on the

variation of intensity of turbulence is confined to x/D values less than 2.0. After this distance the variation of the turbulence intensity with distance from the nozzle reverts to the same variation as a jet without screens (see ref. 6). The intensity levels, however, have been changed by the presence of the screens.

It is not unreasonable that some of the values of the intensity are less than those measured for a jet without screens. The effect of the fine-mesh screen (0.119 in.), which shows lower levels, may perhaps be an example of reduction of the turbulence level by fine-mesh screens as discussed in reference 10. The increase of turbulence intensity with distance from the nozzle exit x/D will probably be arrested within the next diameter or so from the nozzle exit as it is in jets without screens (ref. 6). But no data were taken with screens at $x/D > 5.0$.

Figure 10 shows the relation of turbulence intensity to mesh size and distance from the nozzle exit. This figure gives u'/U_c as a function of mesh size more completely than figure 7.

Spectral Analysis

The spectral density of the turbulent velocities is given in figures 11 and 12 for three different mesh sizes and for x/D values of 1.0, 2.0, 3.0, 4.0, and 5.0 along the jet centerline. The spectral peaks shown in figures 11(a) and (b) and 12(b), (c), and (d) are for the fine- and medium-mesh screens. Large-mesh screens damp out the peaks. These peaks, which occur in the frequency range of 630 to 800 cycles per second, are the result of specific vortex shedding frequencies from the lips of the jet nozzle. The frequency of the vortices can be calculated from known relations on vortex shedding and give, for the present nozzle and air velocity, about 700 cycles per second (ref. 18). These characteristic peaks are most evident from x/D values of 2.0 to 4.0. They are not detected by the hot wire on the axis of the jet ($z/D = 0$) at x/D values less than 2.0, and at larger distances vortices shed from both lips are detected. These vortices are damped out downstream after the core of the jet has been dissipated and the jet turbulence has fully developed.

Another observation about the spectral-density curves is the distribution of energy in the low- and high-frequency bands as shown in particular by figure 12(c). In this case as the distance from the jet increases, a redistribution of energy occurs. For example, at $x/D = 1.0$ and for frequencies less than 1000 cycles per second, the power-spectral-density is about half of that at $x/D = 5.0$. But at frequencies greater than 1000 cycles per second, the reverse is true with level greater for positions close to the nozzle exit as compared with those farther downstream. For the jet without screens (ref. 6) this redistribution does not occur. This result suggested the use of screens as a method of

7. Ribner, H. S., and Tucker, M.: Spectrum of Turbulence in a Contracting Stream. NACA Rep. 1113, 1953. (Supersedes NACA TN 2606.)

8. Tyler, John M., and Perry, Edward C.: Jet Noise. Preprint No. 287, SAE, 1954.

9. Lee, R., and Smith, E. B.: Noise Measurements of Subsonic Concentric Jets. Jour. Acoustic Soc. Am., vol. 29, no. 6, June 1957, p. 779.

10. Dryden, Hugh L., Schubauer, G. B., Mock, W. C., Jr., and Skramstad, H. K.: Measurements of Intensity and Scale of Wind-Tunnel Turbulence and Their Relation to the Critical Reynolds Number of Spheres. NACA Rep. 581, 1937.

11. Coles, Willard D., and North, Warren J.: Screen-Type Noise Reduction Devices for Ground Running of Turbojet Engines. NACA TN 4033, 1957.

12. Callaghan, Edmund E., and Coles, Willard D.: Investigation of Jet-Engine Noise Reduction by Screens Located Transversely Across the Jet. NACA TN 3452, 1955.

13. Laurence, James C., and Landes, L. Gene: Auxiliary Equipment and Techniques for Adapting the Constant-Temperature Hot-Wire Anemometer to Specific Problems in Air-Flow Measurements. NACA TN 2843, 1953.

14. Schubauer, G. B., and Klebanoff, P. S.: Theory and Application of Hot-Wire Instruments in the Investigation of Turbulent Boundary Layers. NACA WR-86, 1946. (Supersedes NACA ACR 5K27.)

15. Carlson, Edward R., et al.: Special Electronic Equipment for the Analysis of Statistical Data. Proc. IRE, vol. 47, no. 5, pt. I, May 1959, pp. 956-962.

16. Taylor, G. I.: Statistical Theory of Turbulence. Pts. I - IV. Proc. Roy. Soc. (London), ser. A, vol. 151, no. A873, Sept. 2, 1935, pp. 421-478; pt. V, ser. A, vol. 156, Aug. 17, 1936, pp. 307-317.

17. Sandborn, Virgil A.: Experimental Evaluation of Momentum Terms in Turbulent Pipe Flow. NACA TN 3266, 1955.

18. Roshko, Anatol: On the Development of Turbulent Wakes from Vortex Streets. NACA Rep. 1191, 1954. (Supersedes NACA TN 2913.)

TABLE I. - DATA ON SCREENS

Mesh size, M, in.	Wire size, d, in.
0.119	0.0318
.252	.0475
.472	.1054

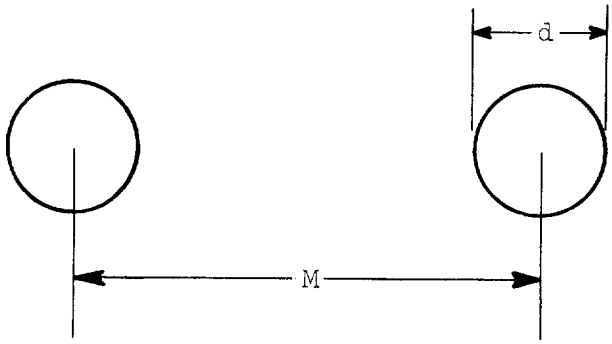

TABLE II. - PRESSURE DROP ACROSS SCREENS

Mesh size, in.	Mach number (a)	$P - P_B$, in. Hg (a)	ΔP, in. Hg	U_l, ft/sec
0.119	0.3	2	1.08	244
.252	.3	2	.80	277
.472	.3	2	.92	263

[a]No screens present.

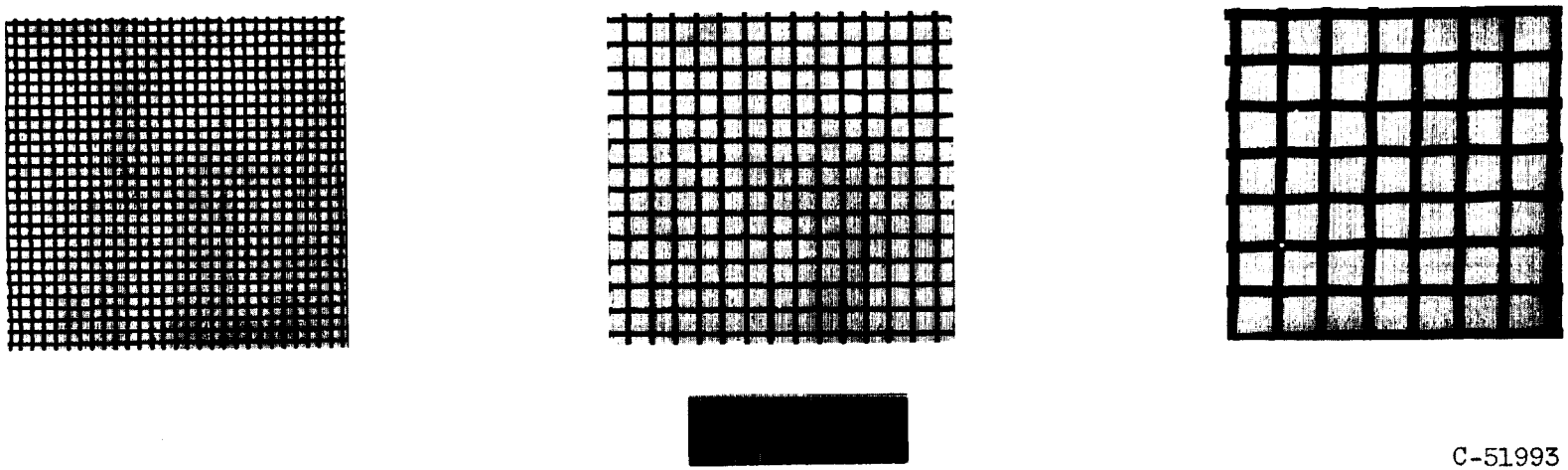

C-51993

Figure 1. - Screens used in experiment.

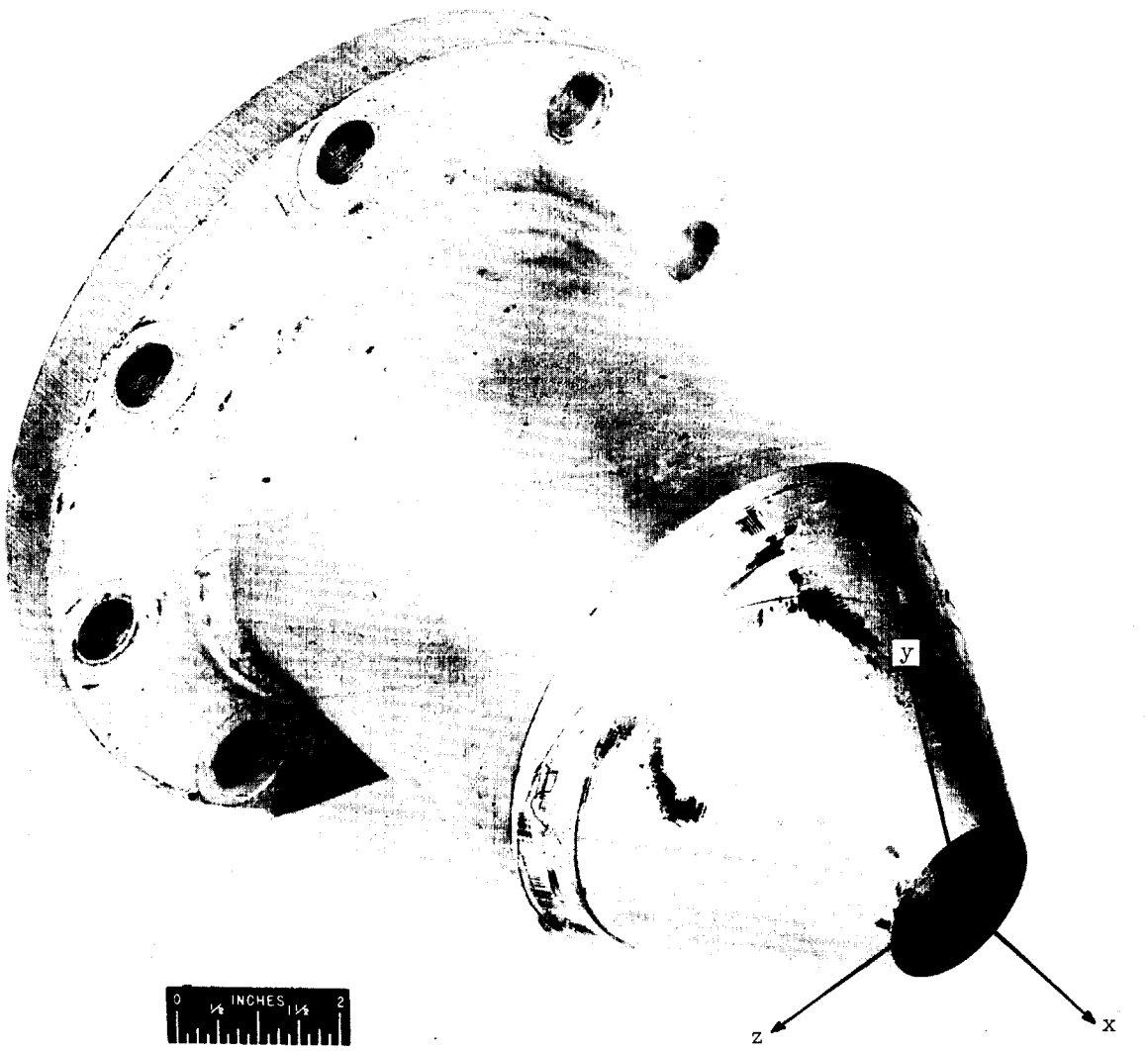

Figure 2. - Convergent nozzle and coordinate system.

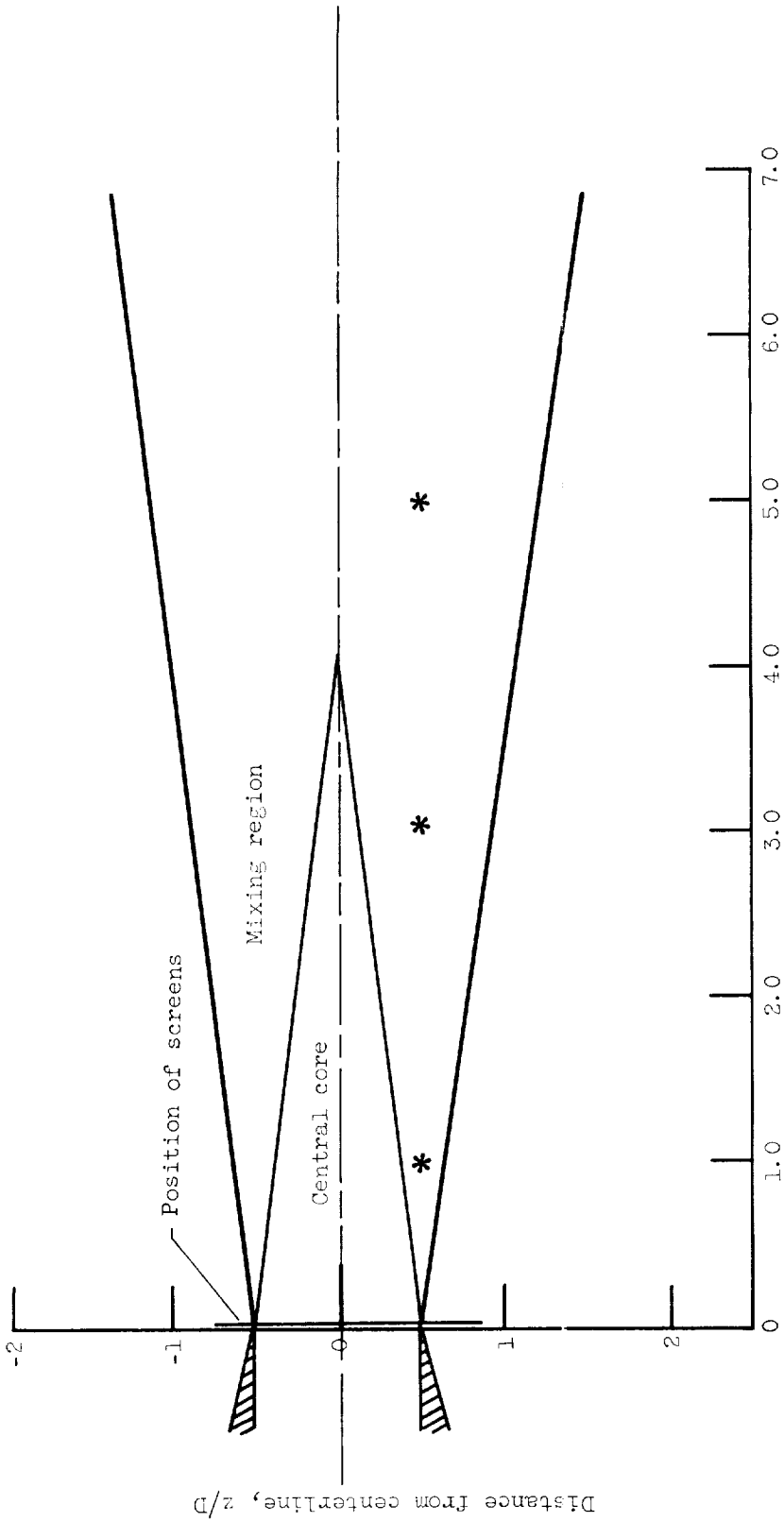

Figure 3. - Measuring stations in air jet.

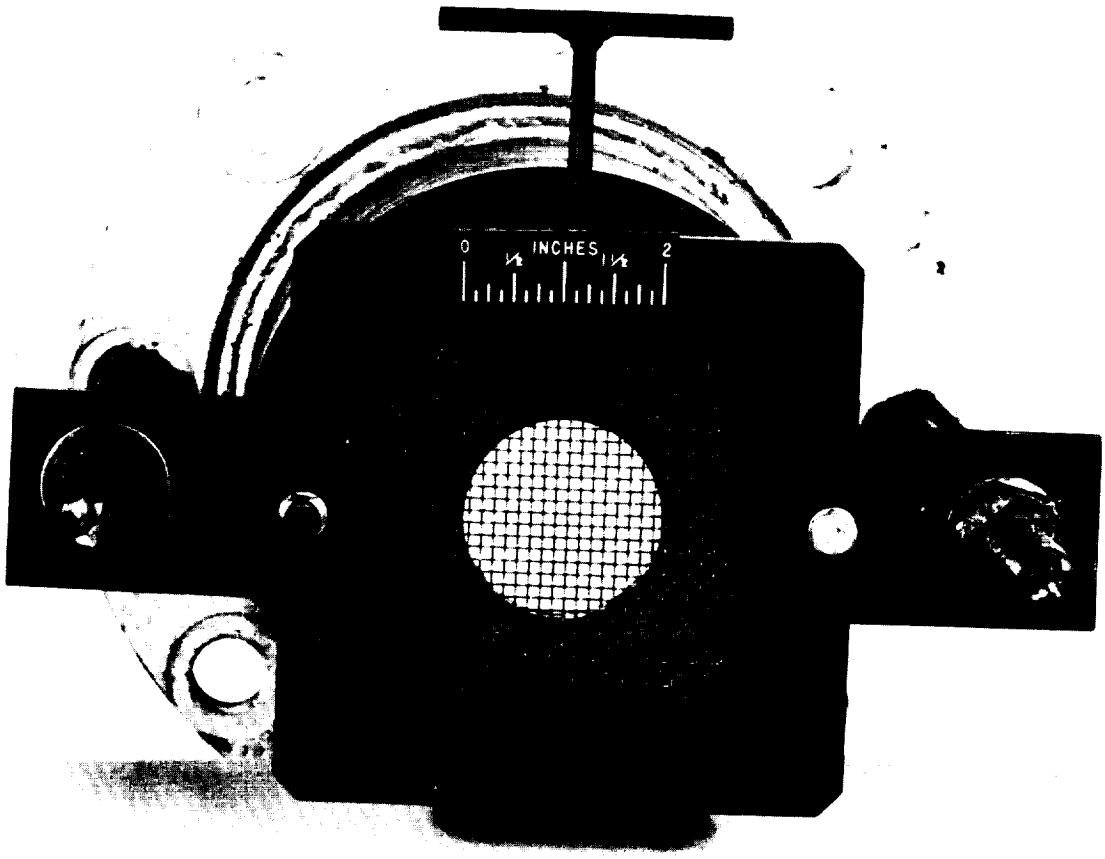

C-51994

Figure 4. - Screen holder bolted to nozzle.

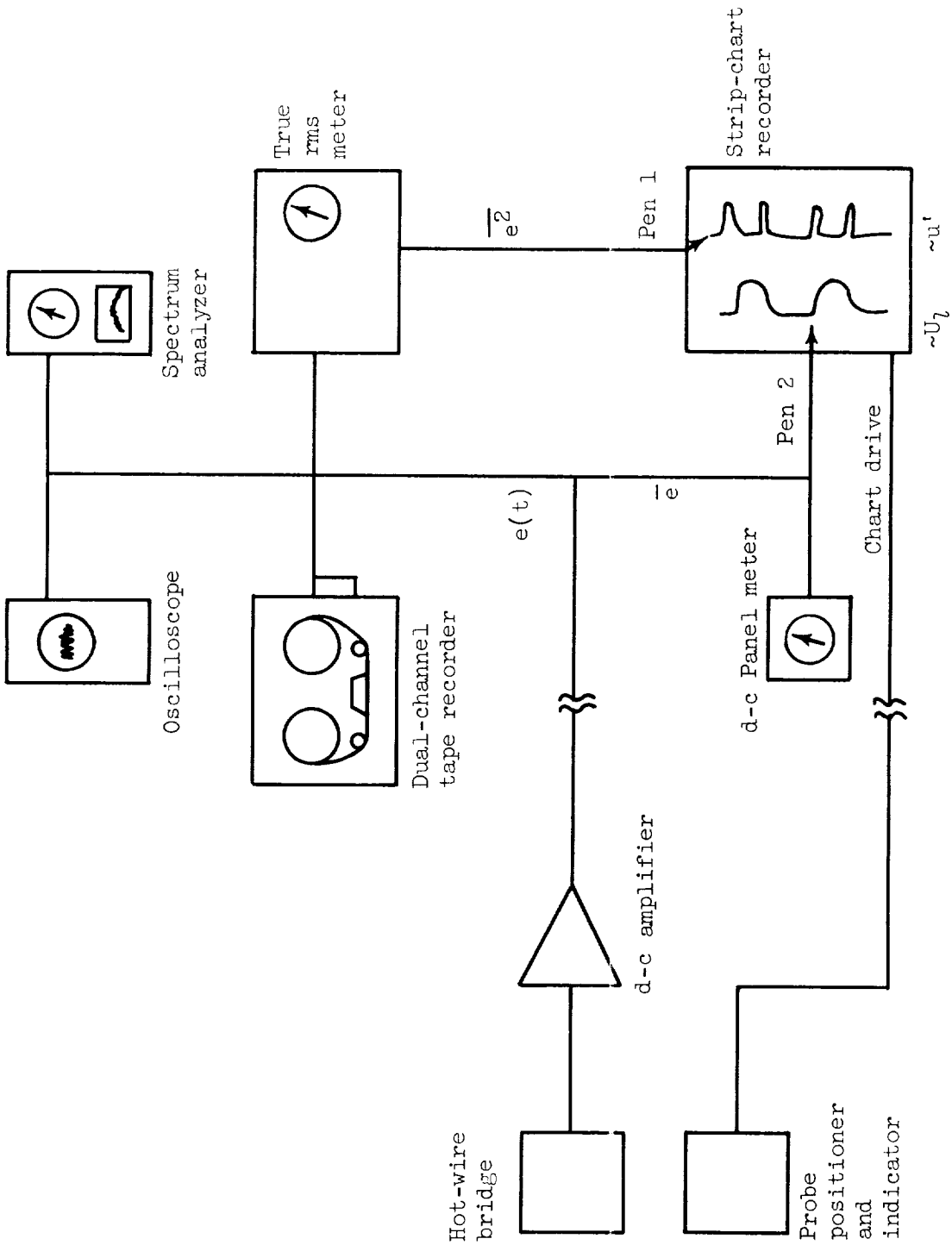

Figure 5. - Block diagram of instrumentation.

E-798

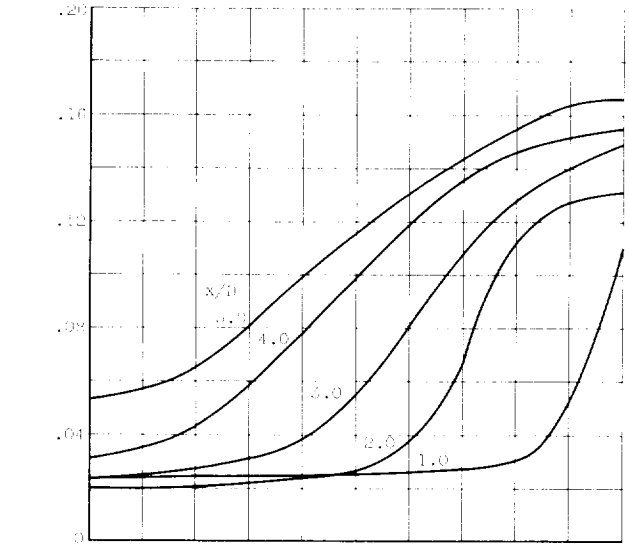

(a) Mesh size, 0.119 inch.

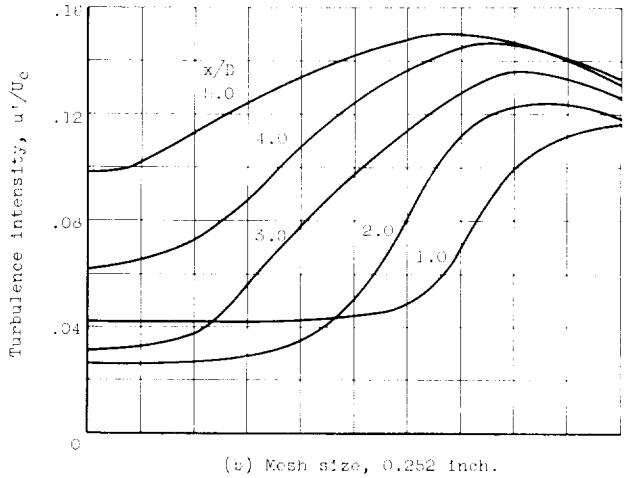

(b) Mesh size, 0.252 inch.

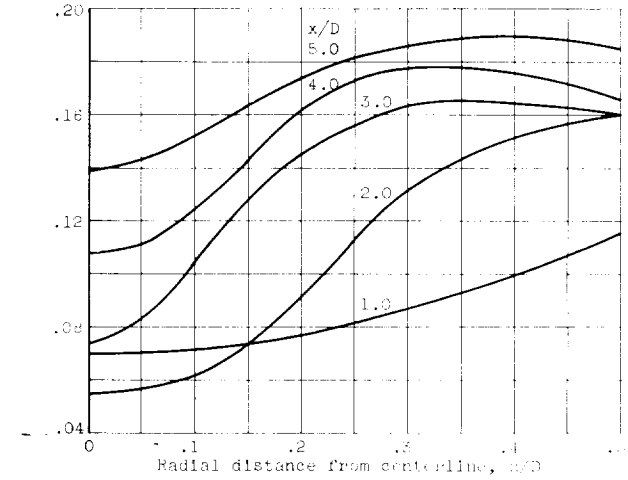

(c) Mesh size, 0.472 inch.

Figure 6. - Intensity of turbulence as function of distance from jet centerline.

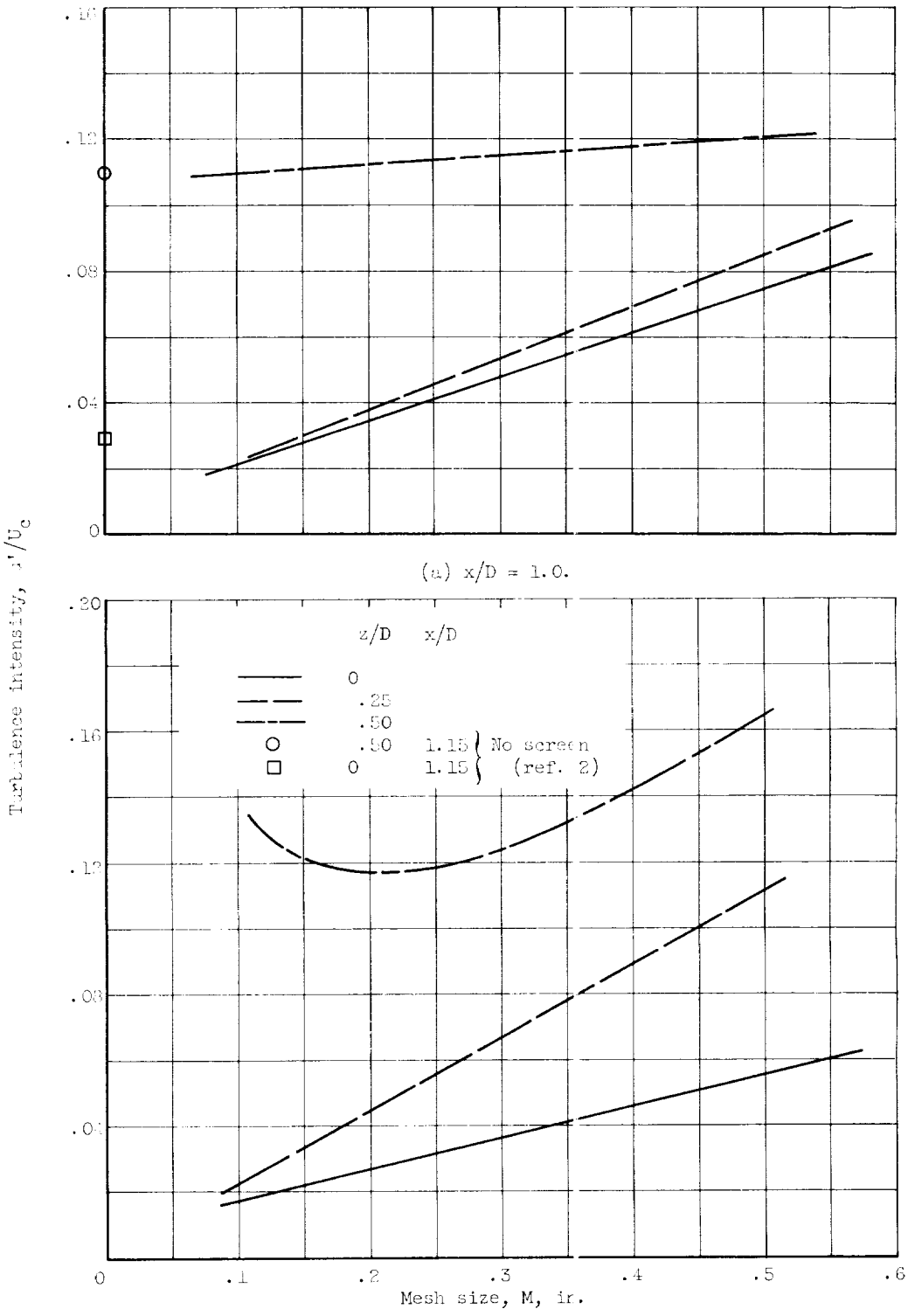

Figure 7. - Intensity of turbulence as function of screen mesh size.

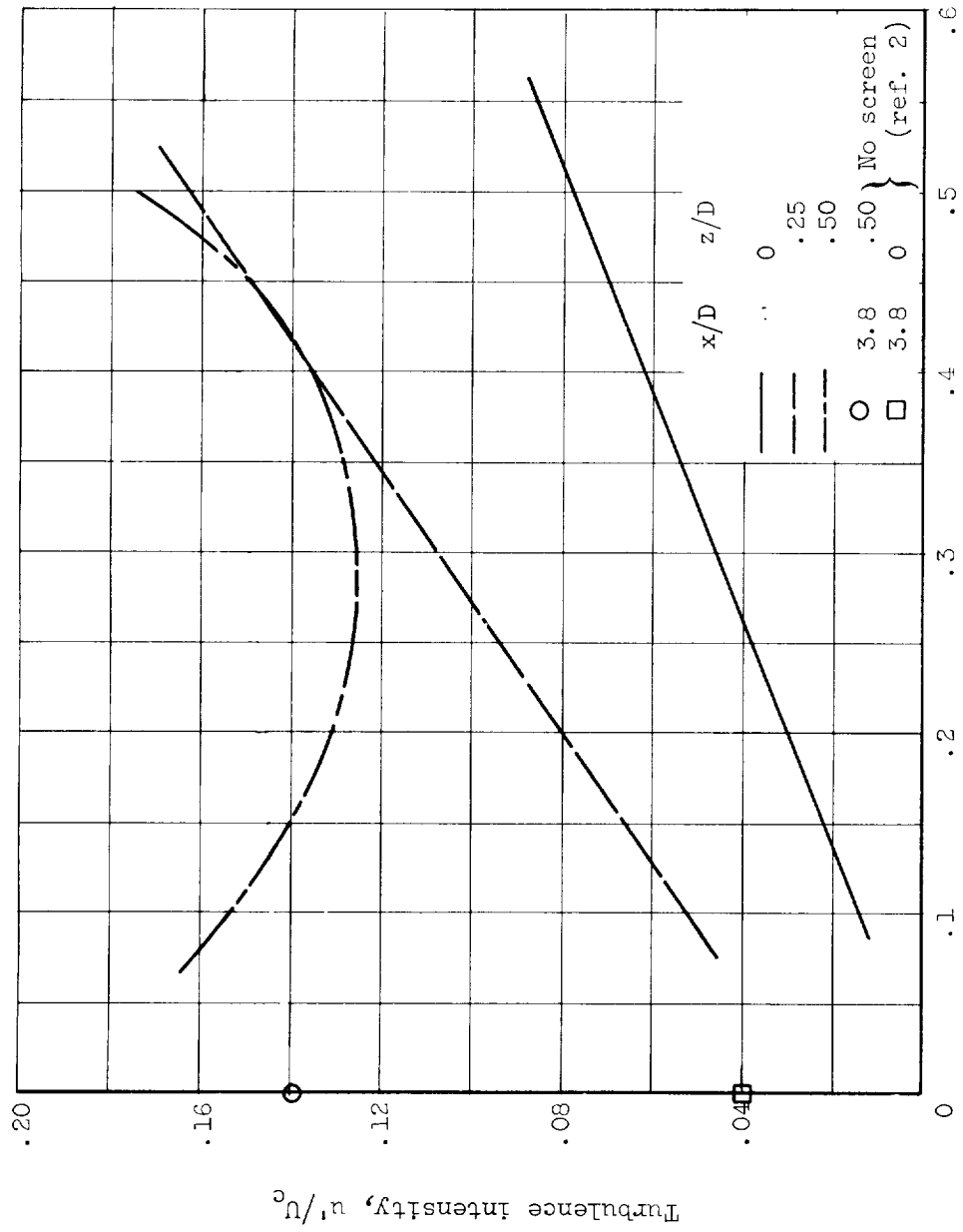

(c) $x/D = 3.0$.

Figure 7. - Continued. Intensity of turbulence as function of screen mesh size.

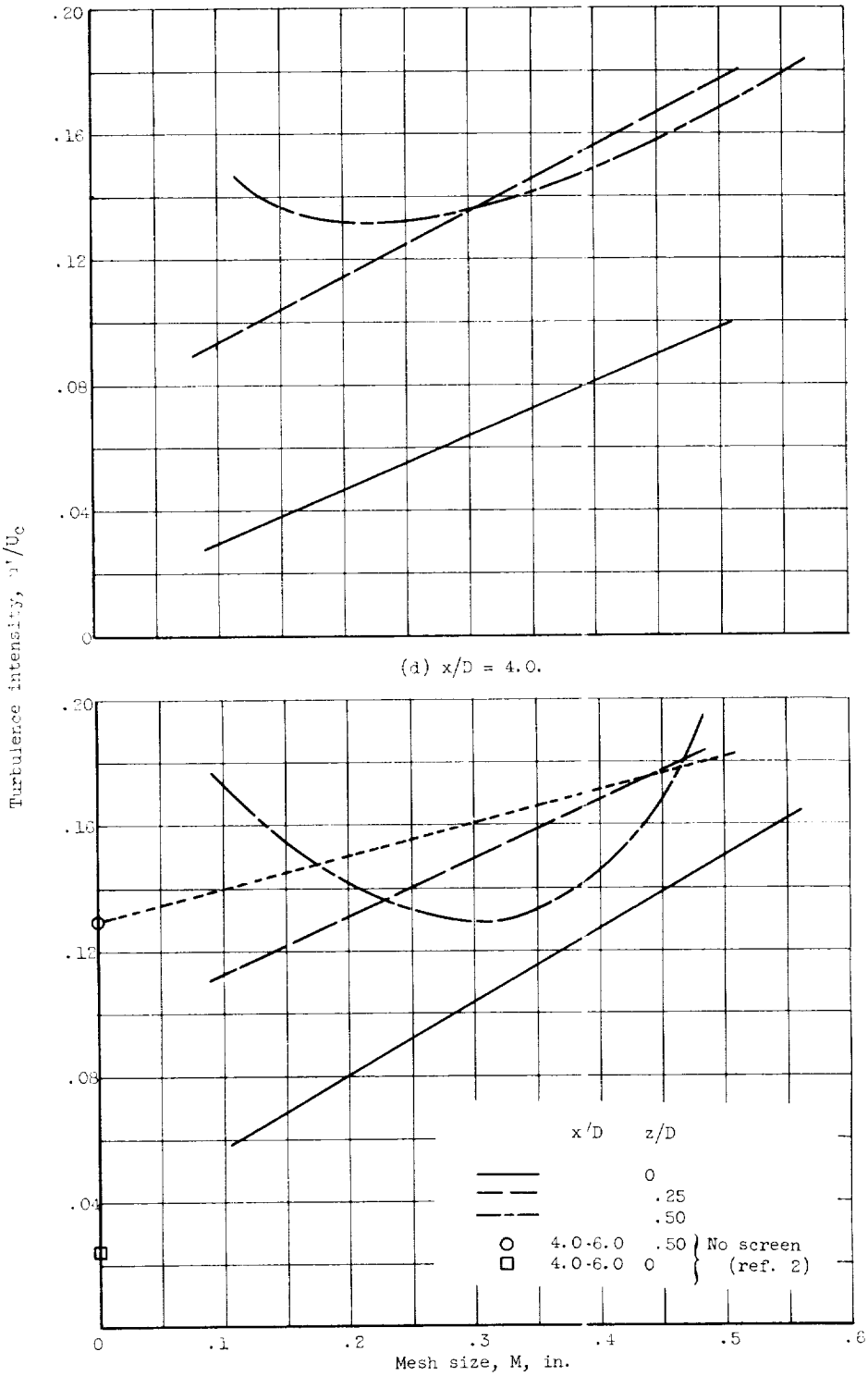

Figure 7. - Concluded. Intensity of turbulence as function of screen mesh size.

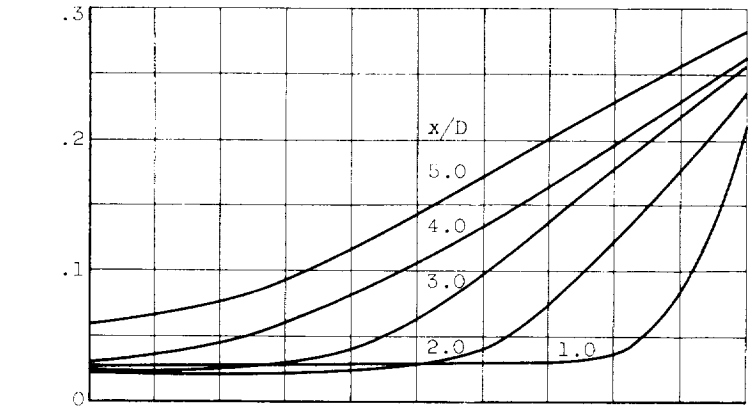

(a) Mesh size, 0.119 inch.

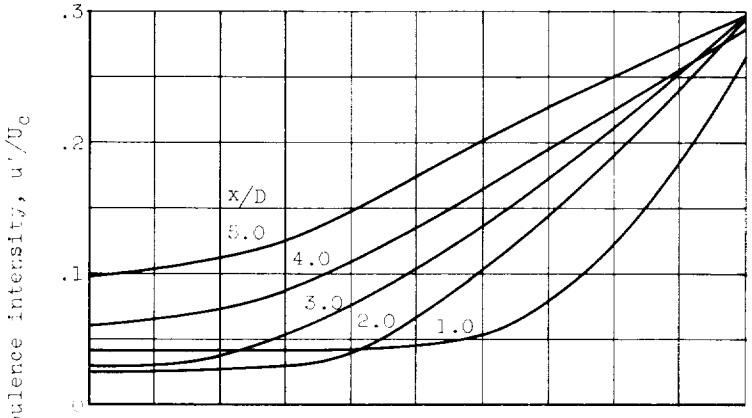

(b) Mesh size, 0.252 inch.

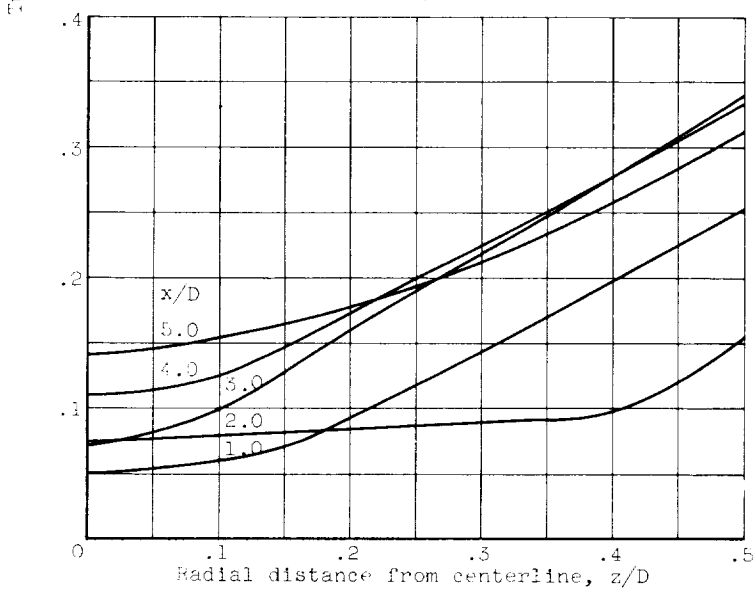

(c) Mesh size, 0.472 inch.

Figure 8. - Intensity of turbulence as function of radial distance from jet centerline.

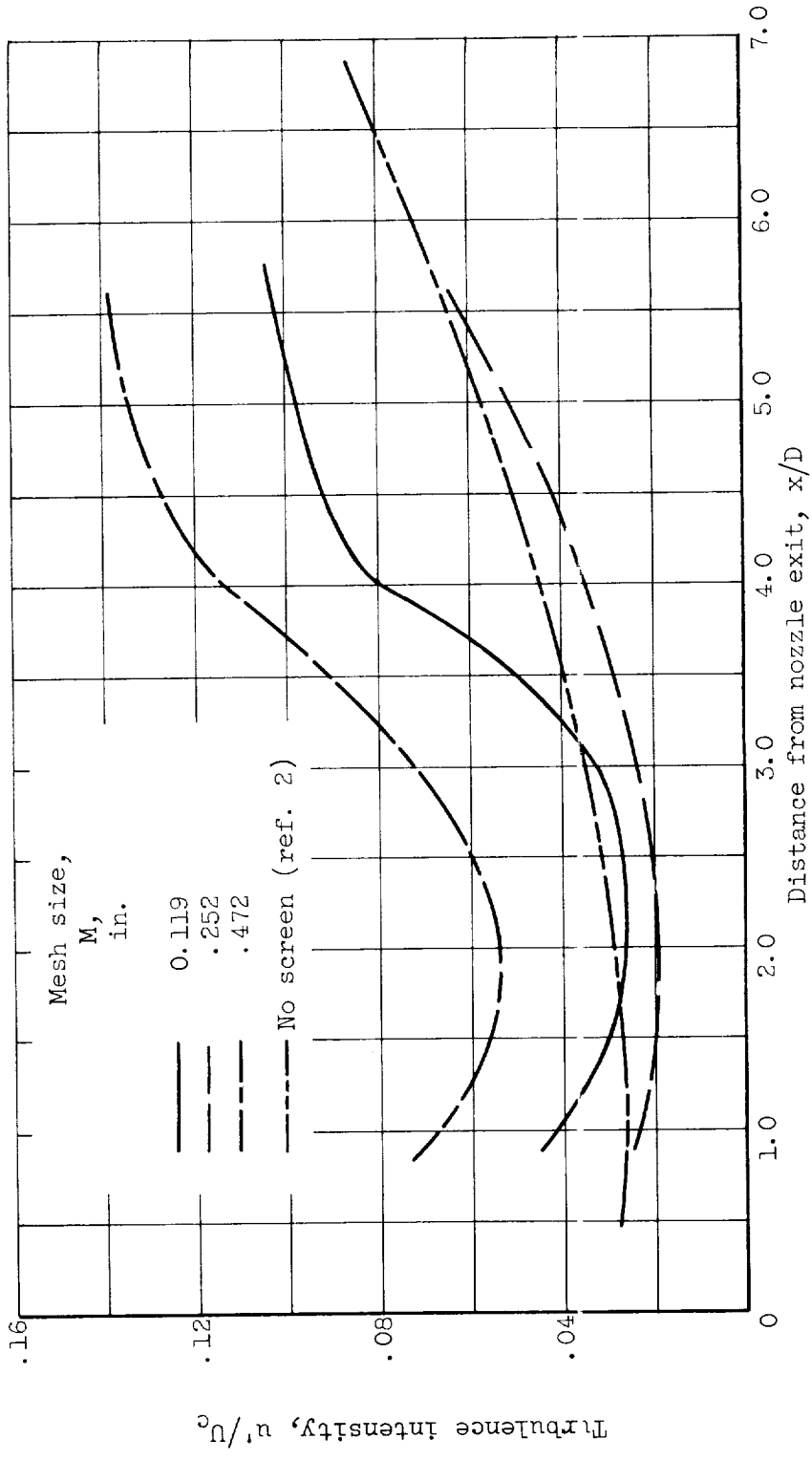

Figure 9. - Intensity of turbulence as function of distance from nozzle exit. z/D = 0.

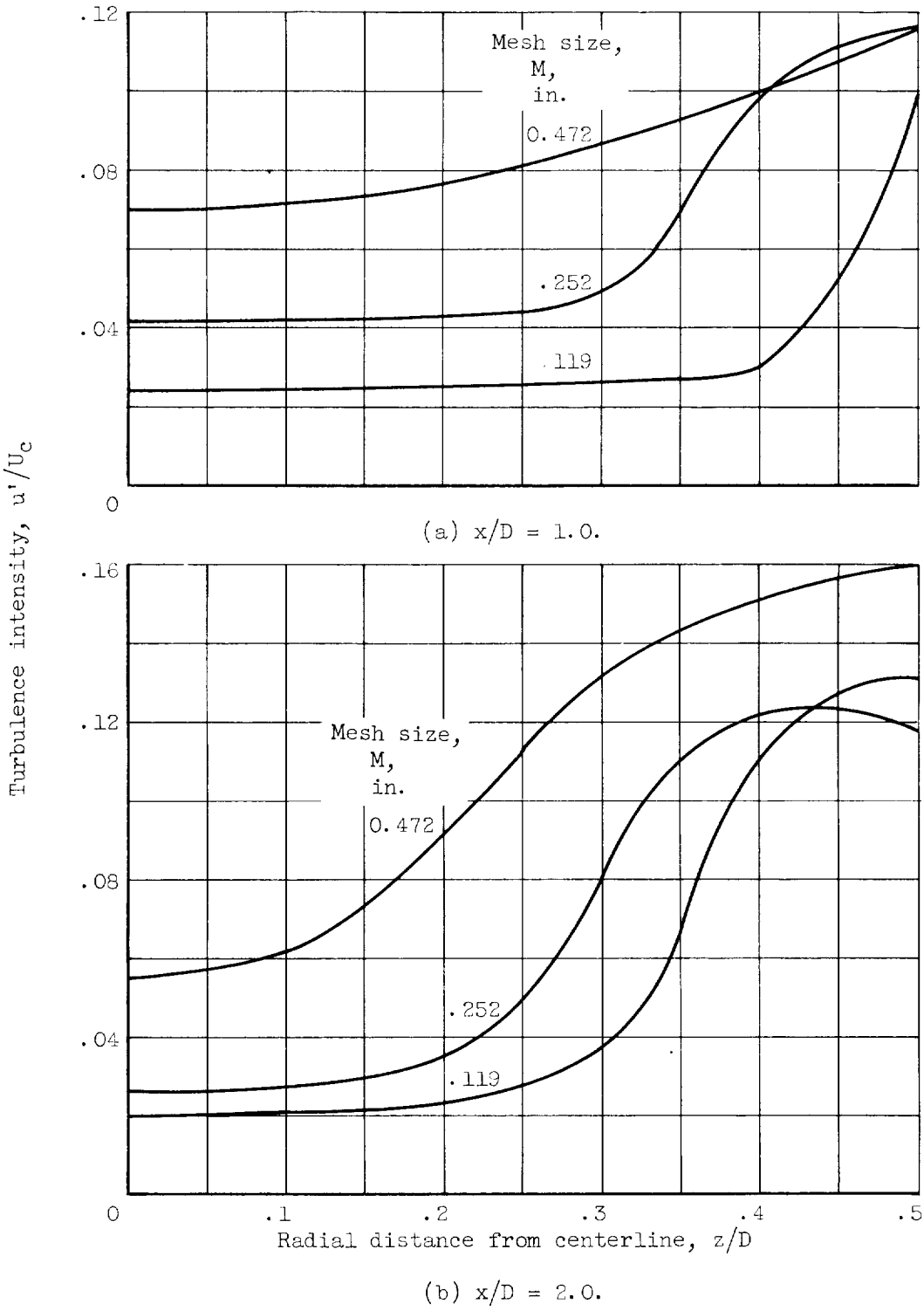

Figure 10. - Intensity of turbulence as function of mesh size and distance from nozzle exit.

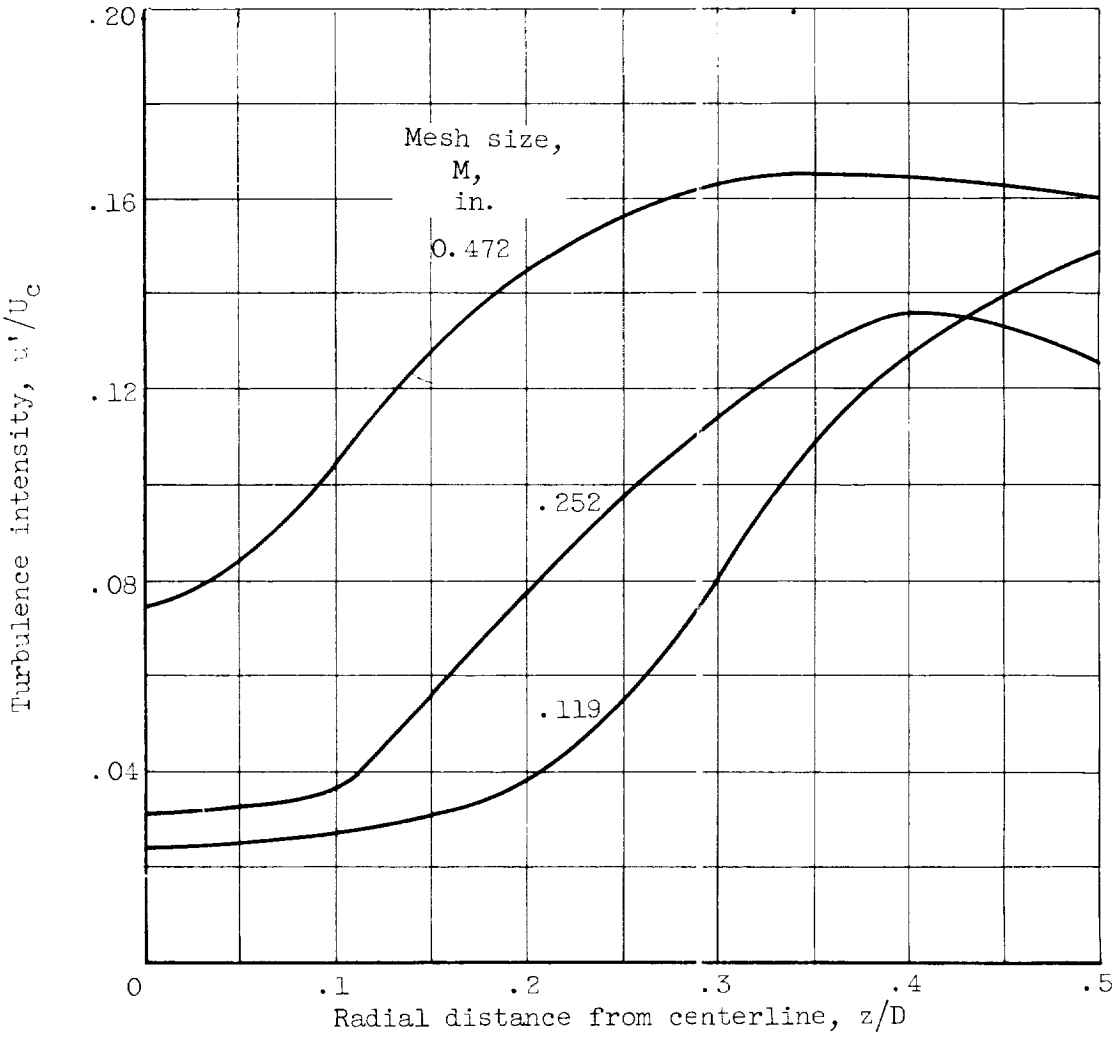

(c) x/D = 3.C.

Figure 10. - Continued. Intensity of turbulence as function of mesh size and distance from nozzle exit.

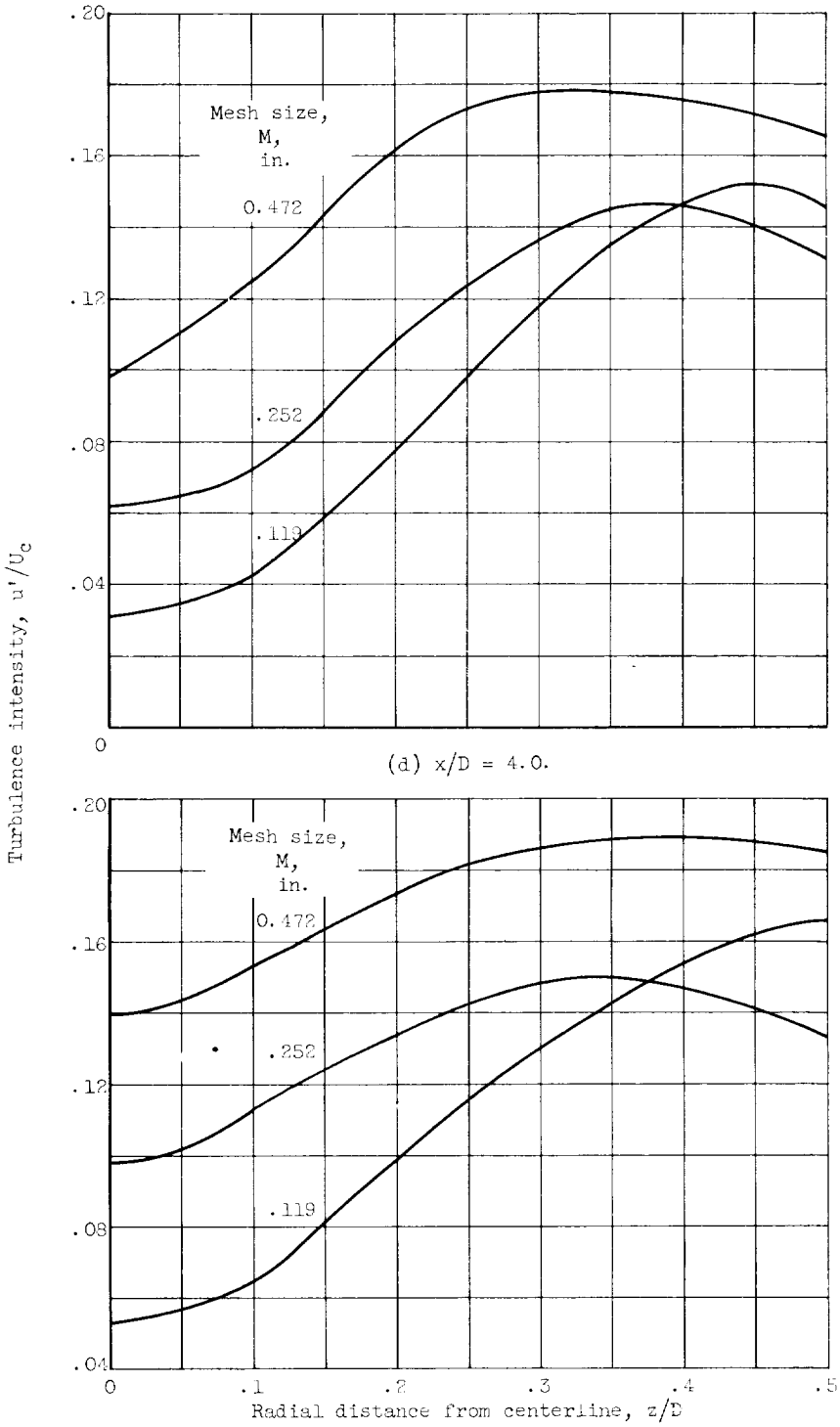

Figure 10. - Concluded. Intensity of turbulence as function of mesh size and distance from nozzle exit.

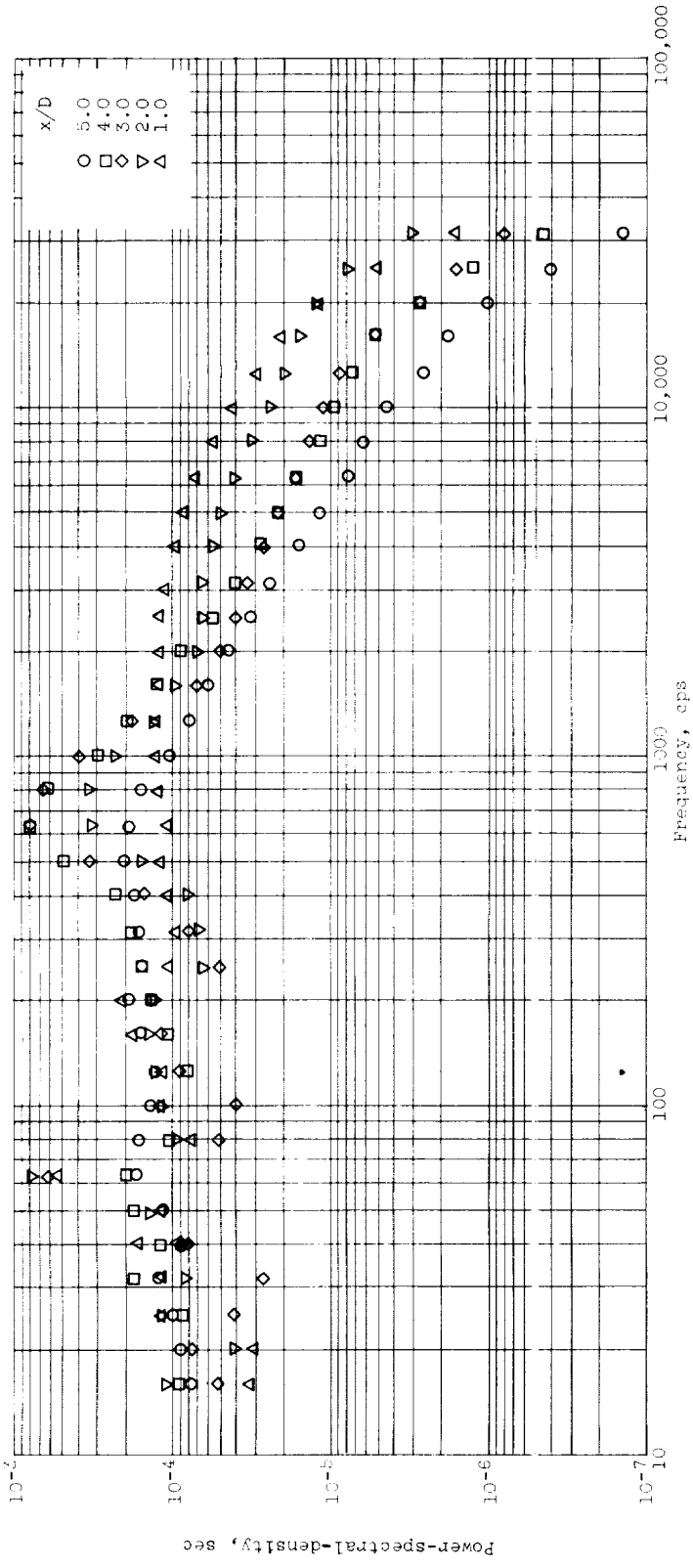

(a) Mesh size, 0.113 inch.

Figure 11. - Spectrum of turbulence as function of distance from nozzle exit. y/D = 0; z/D = 0.

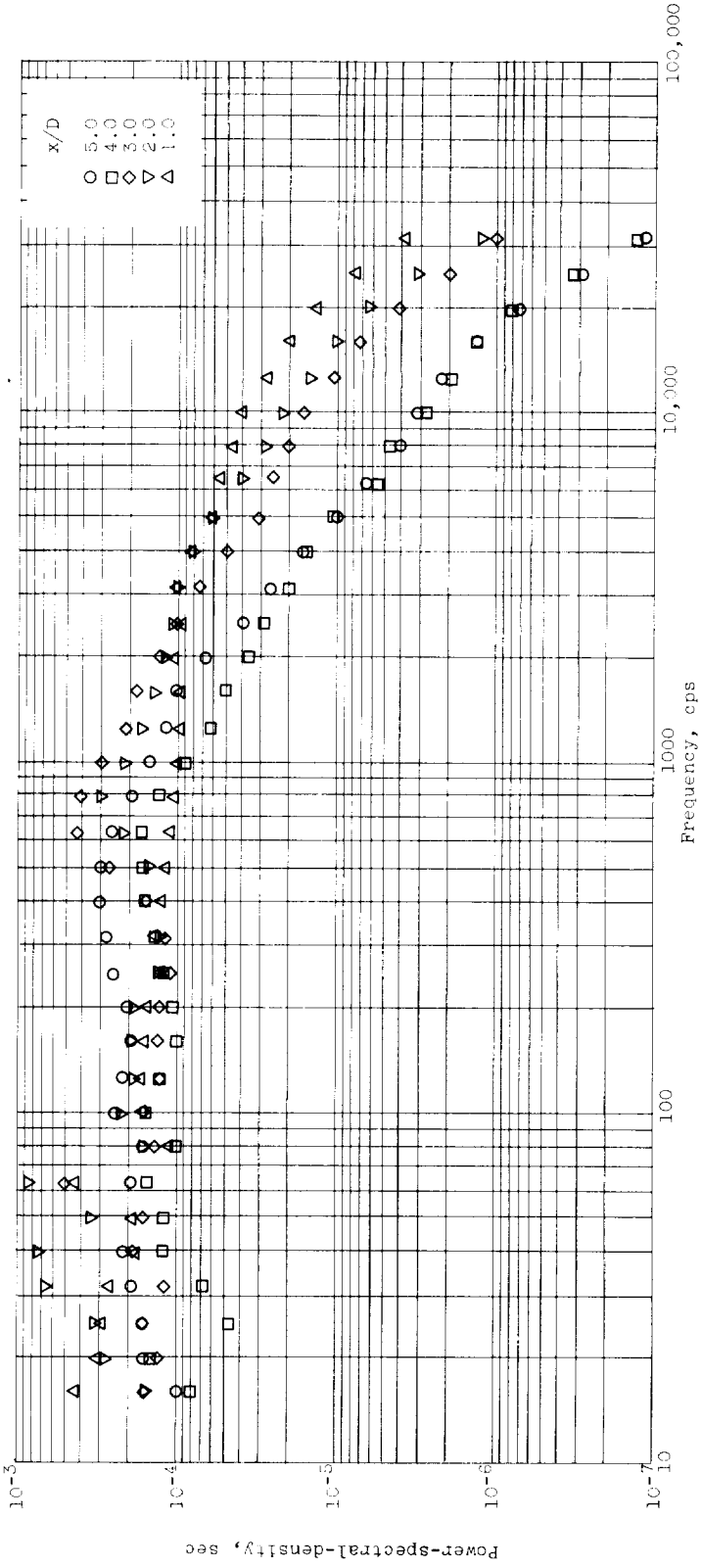

(c) Mesh size, 0.252 inch.

Figure 11. - Continued. Spectrum of turbulence as function of distance from nozzle exit. $x/D = 0$; $z/D = 0$.

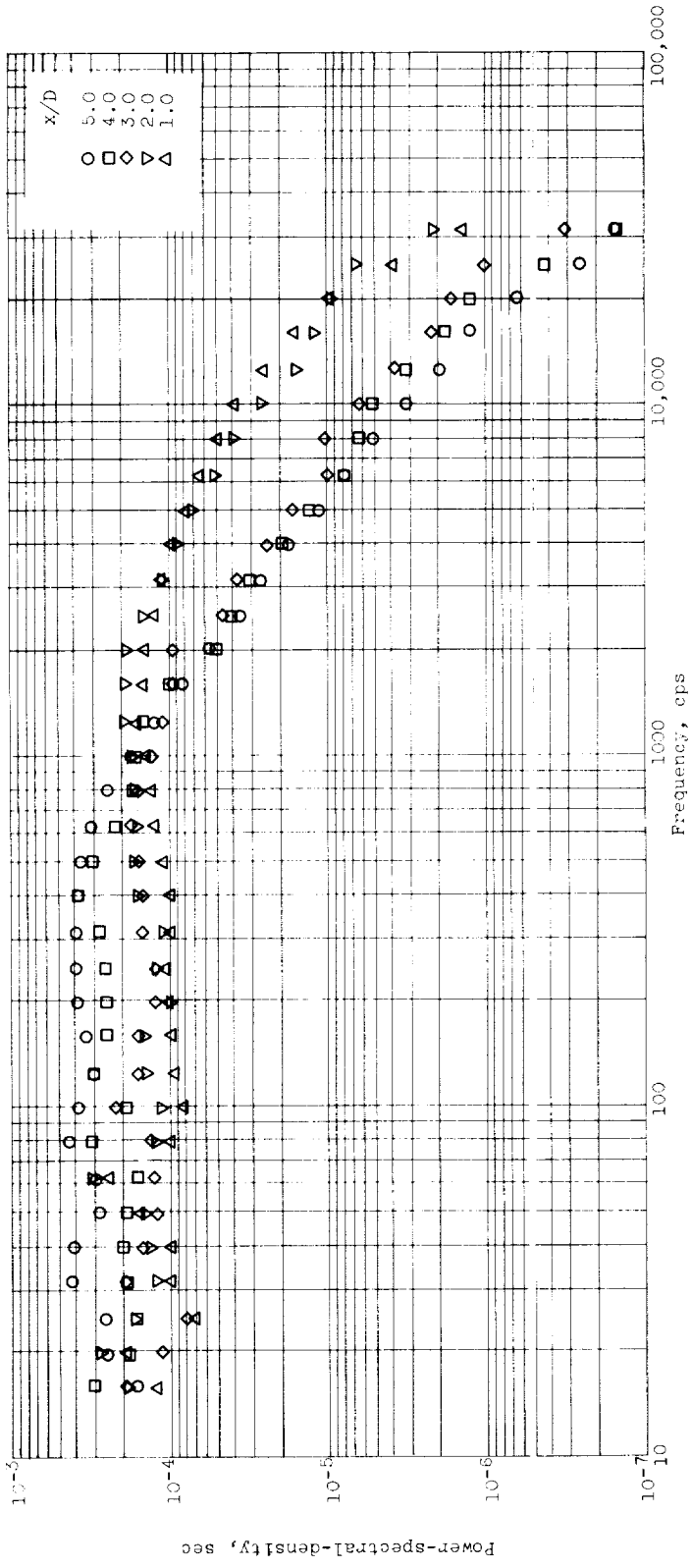

(c) Mesh size, 0.472 inch.

Figure 11. - Concluded. Spectrum of turbulence as function of distance from nozzle exit, y/D = 0; z/D = 0.

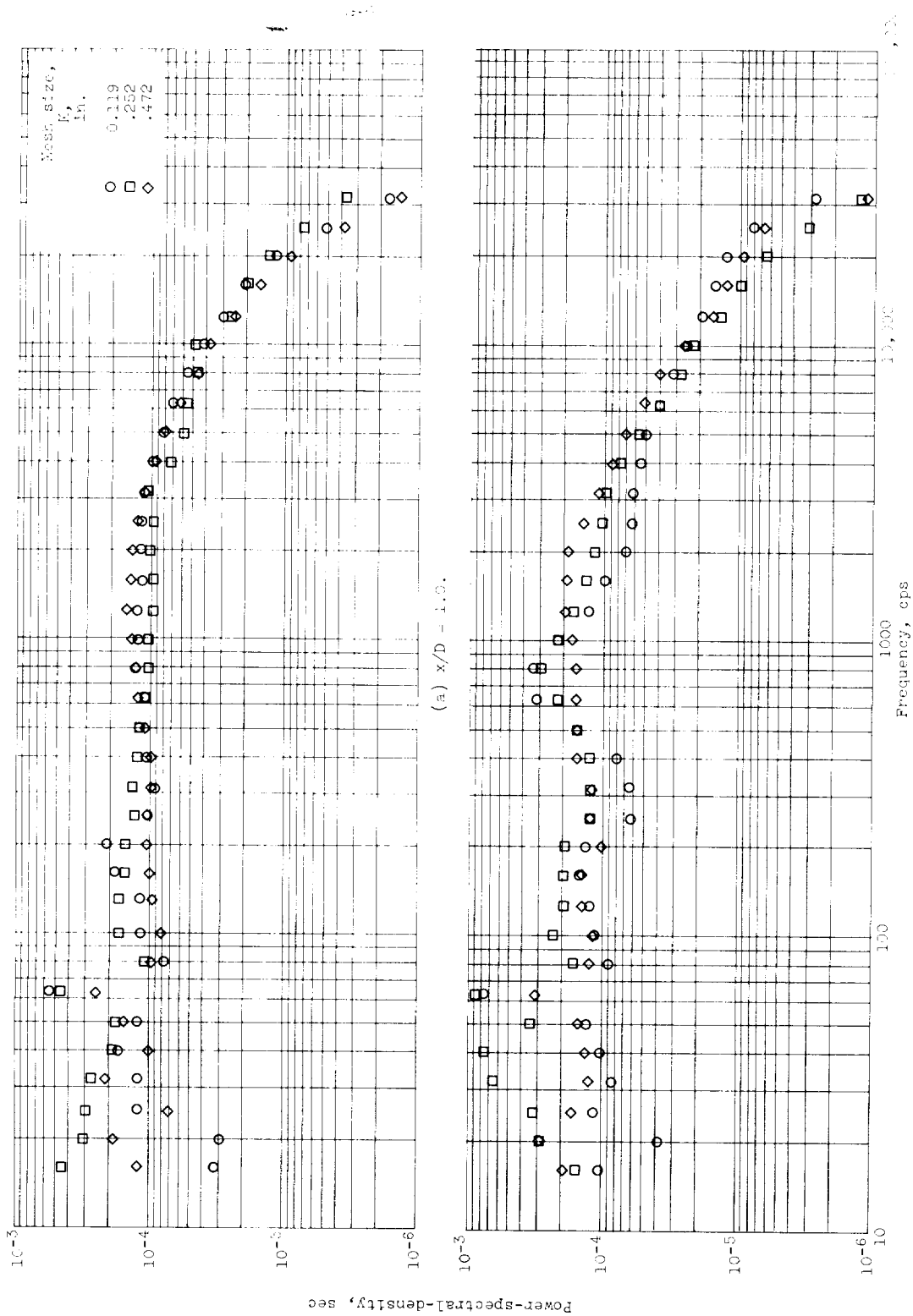

Figure 12. - Power-spectral-density as function of mesh size. y/D = 0; z/D = 0.

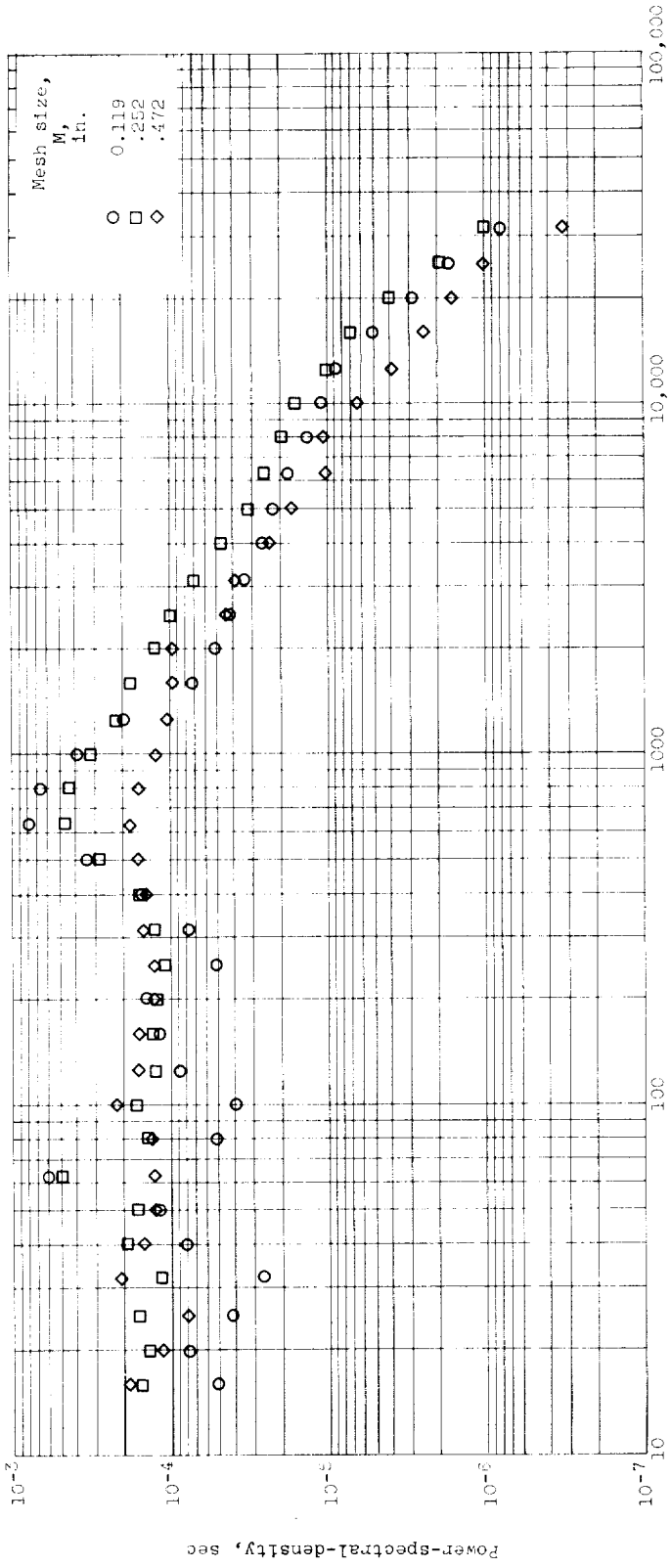

(c) x/D = 5.0.

Figure 12. - Continued. Power-spectral-density as function of mesh size. y/D = 0; z/D = 0.

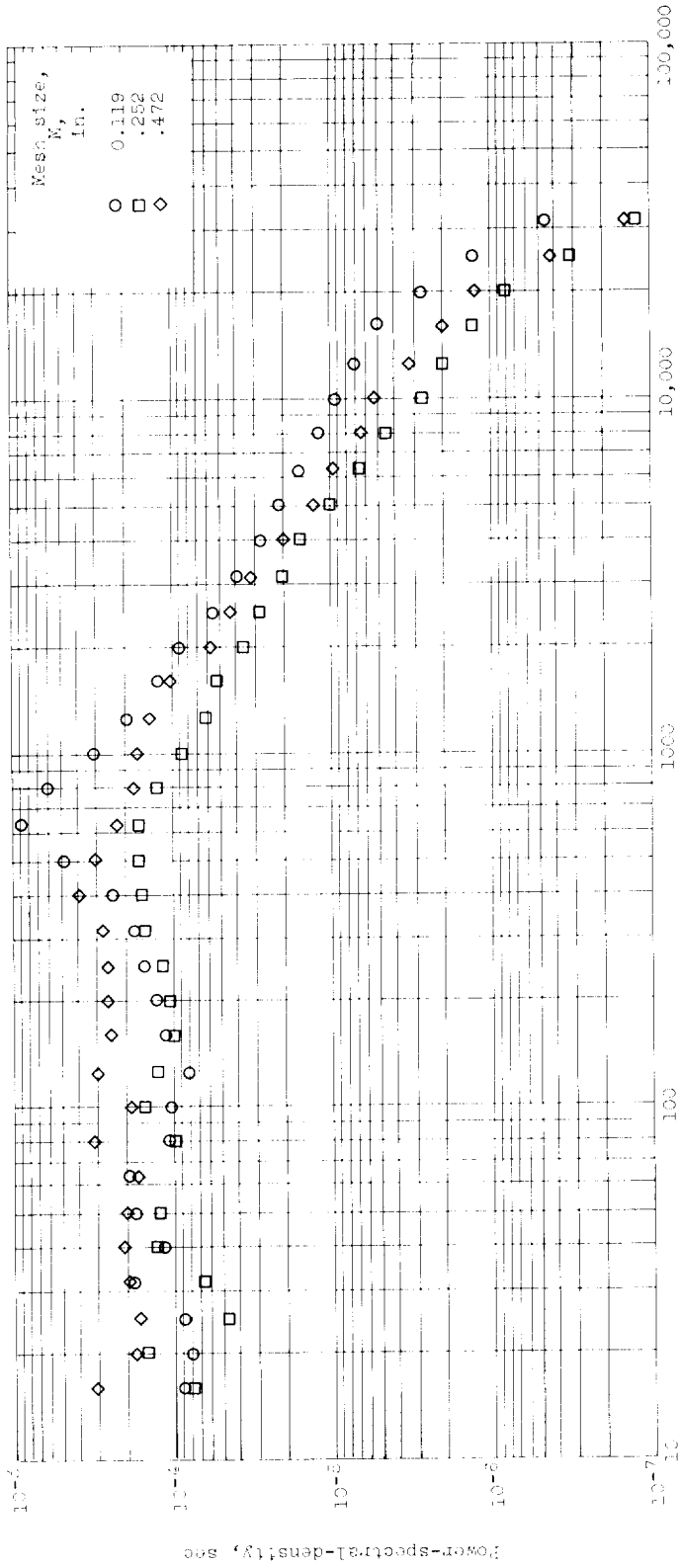

(d) x/D = 4.0.

Figure 12. - Continued. Power-spectral-density as function of mesh size. y/D = 0; z/D = 0.

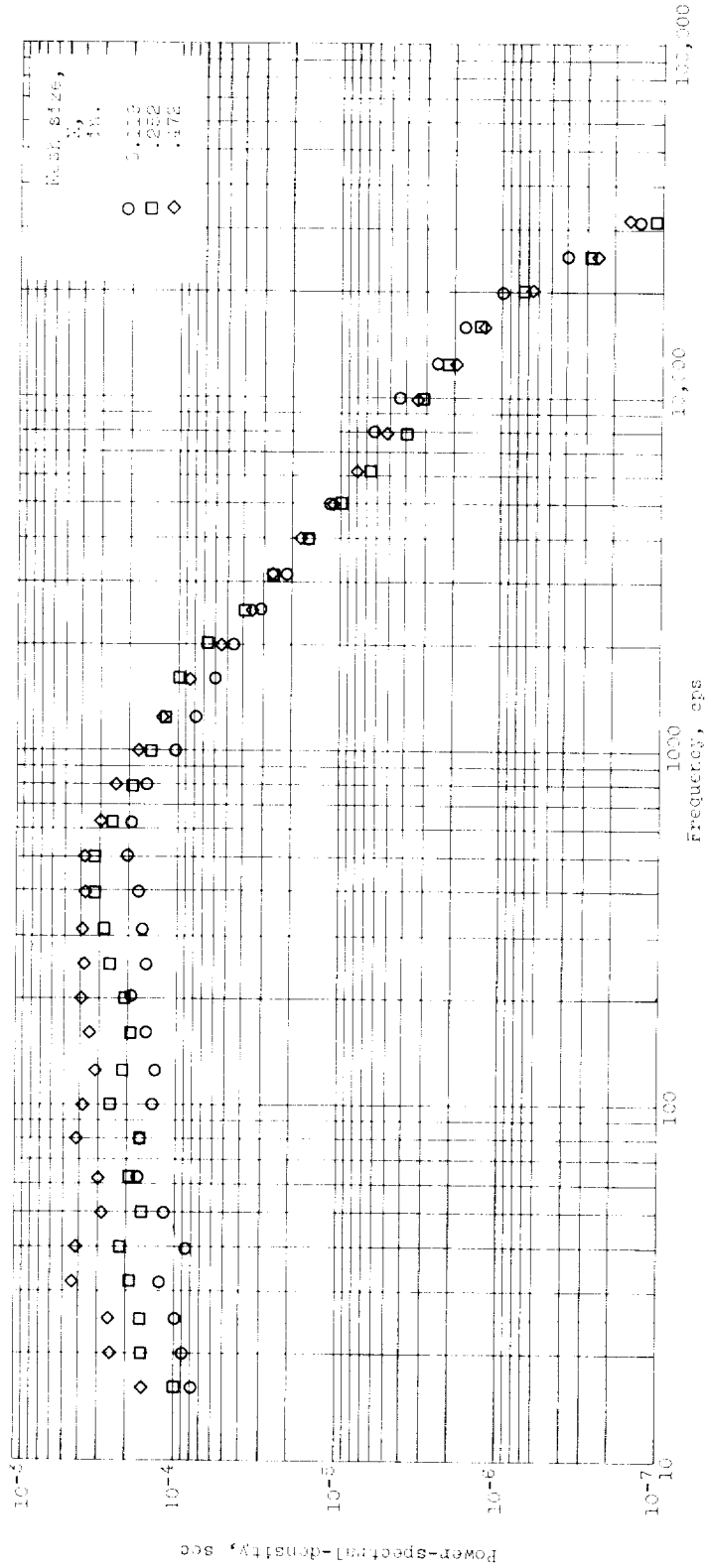

(e) x/D = 4.0.

Figure 12. - Concluded. Power-spectral-density as function of mesh size. y/D = 0; z/D = 0.

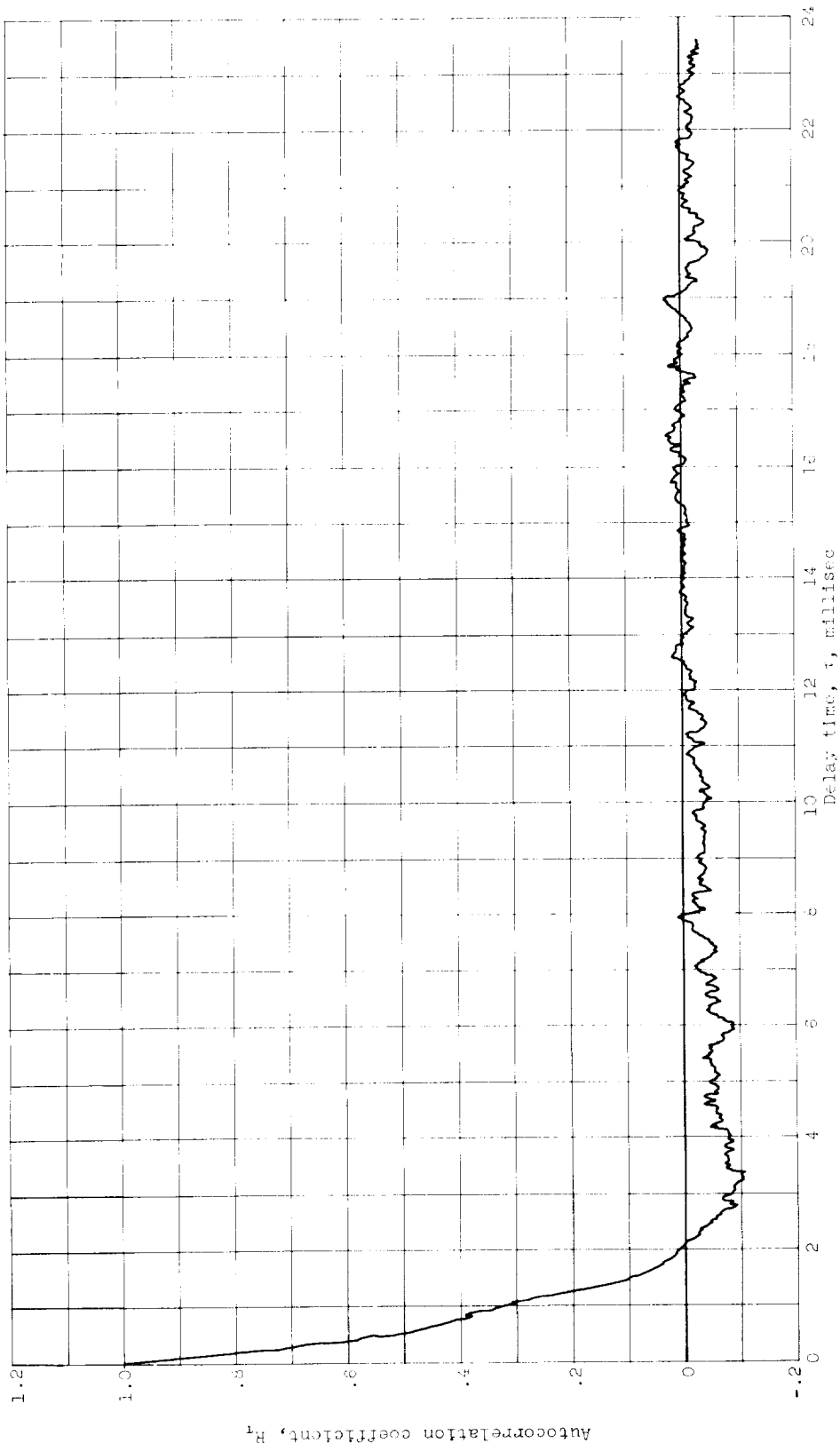

Figure 13. - Experimental autocorrelogram. x/D = 8.0; mesh size, 0.172 inch.

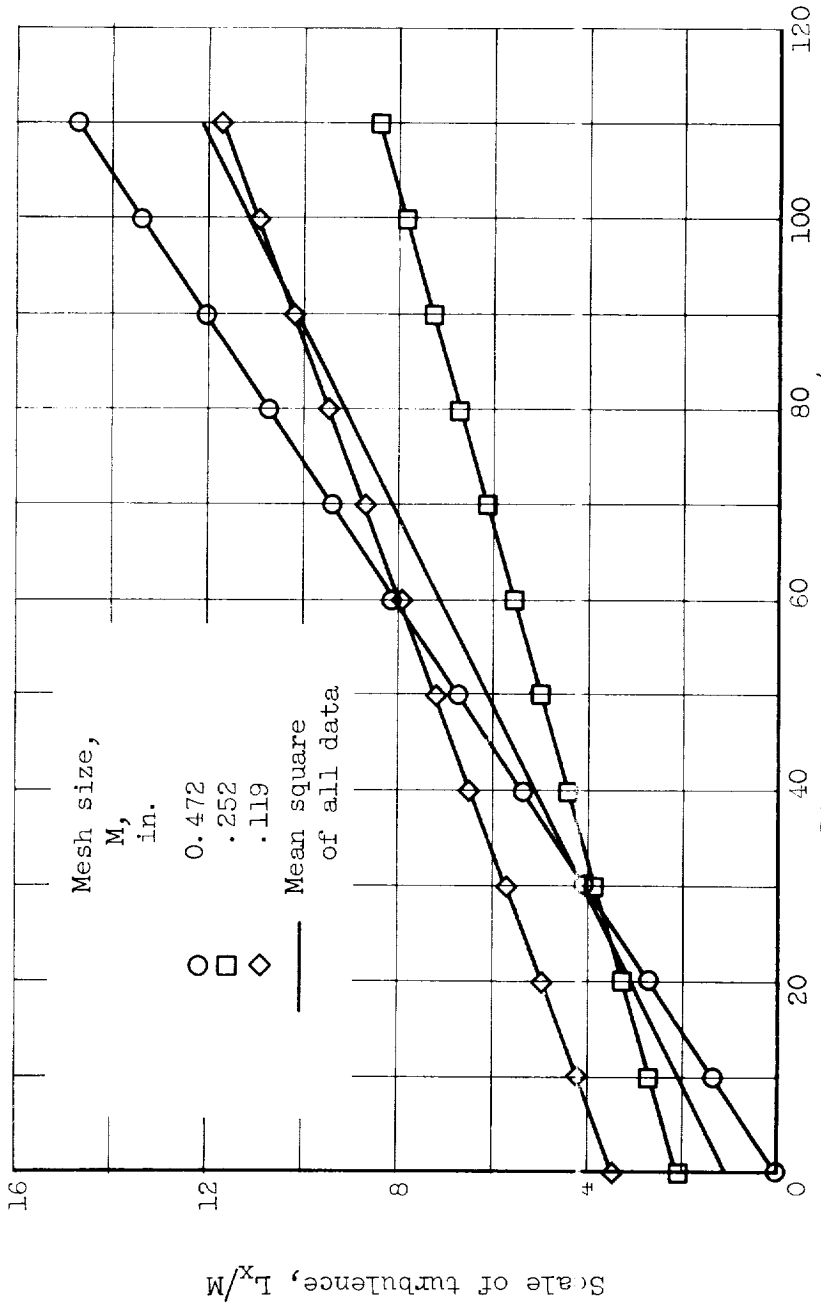

Figure 14. - Scale of turbulence as function of distance from nozzle exit.

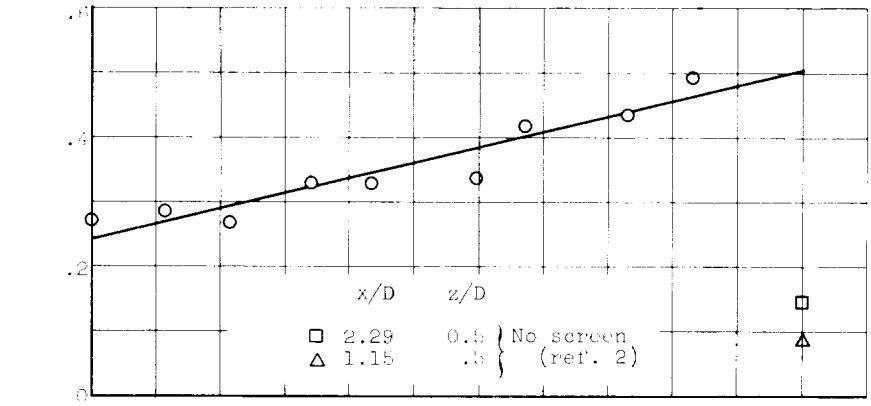

(a) x/D = 2.0; mesh size, 0.119 inch.

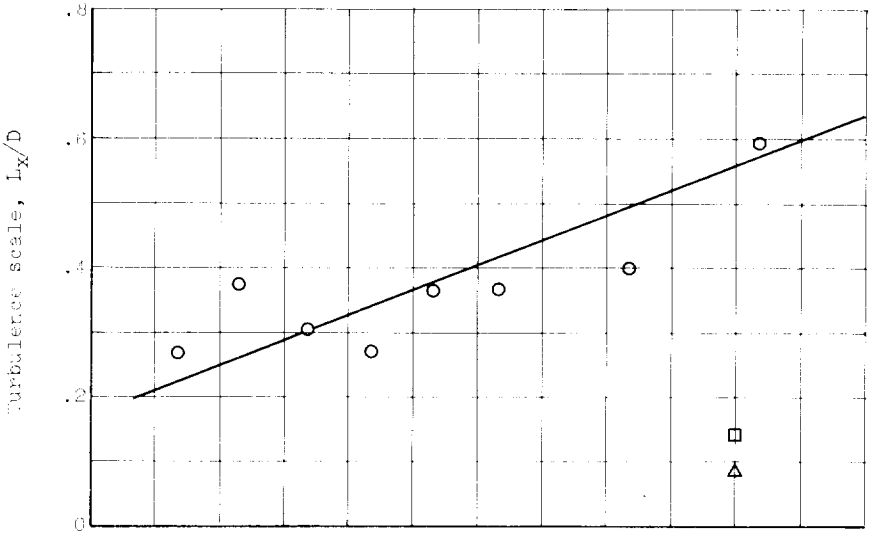

(b) x/D = 2.0; mesh size, 0.242 inch.

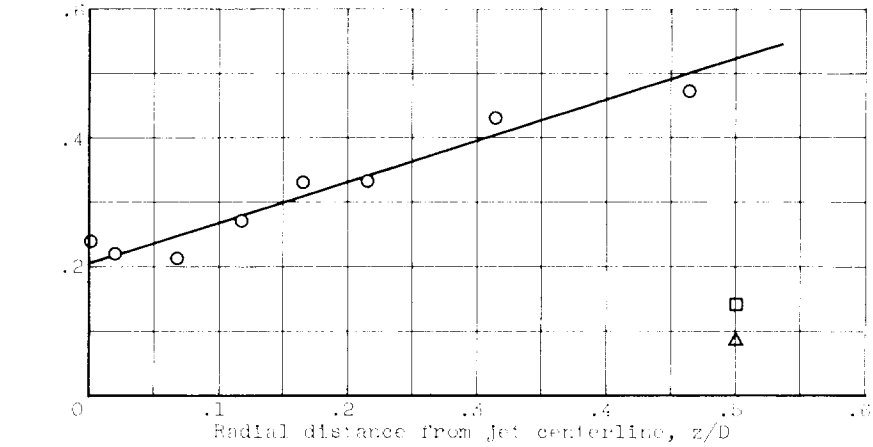

(c) x/D = 2.0; mesh size, 0.472 inch.

Figure 15. - Scale of turbulence as function of radial distance from centerline. y/D = 0.

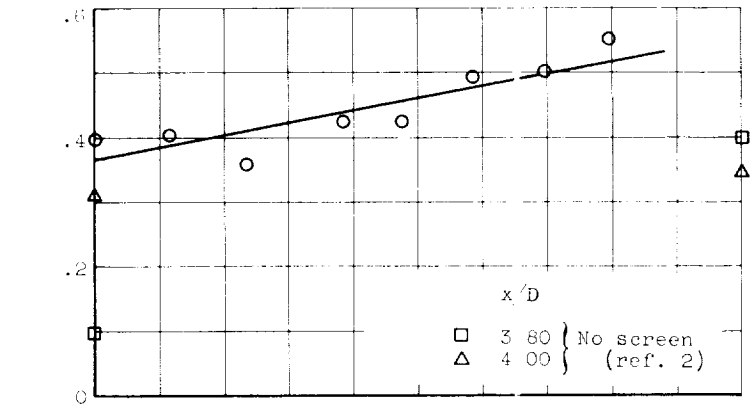

(d) x/D = 3.0; mesh size, 0.119 inch.

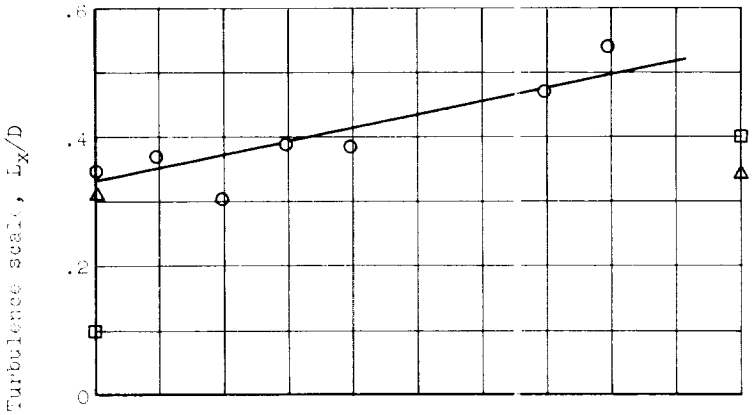

Turbulence scale, L_x/D

(e) x/D = 3.0; mesh size, 0.262 inch.

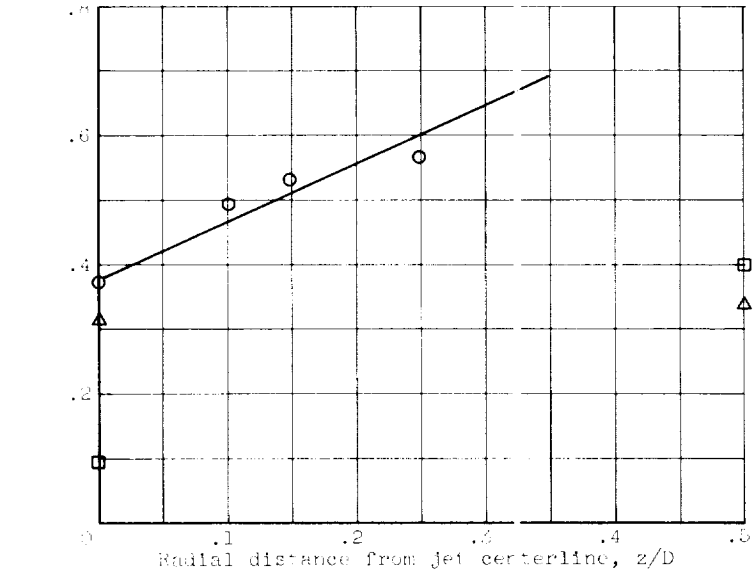

(f) x/D = 3.0; mesh size, 0.472 inch.

Figure 15. - Concluded. Scale of turbulence as function of radial distance from centerline. y/D = 0.